

NASA/TP-2005-213943



# The Effect of Basis Selection on Static and Random Acoustic Response Prediction Using a Nonlinear Modal Simulation

*Stephen A. Rizzi*  
*Langley Research Center, Hampton, Virginia*

*Adam Przekop*  
*National Institute of Aerospace, Hampton, Virginia*

## The NASA STI Program Office . . . in Profile

Since its founding, NASA has been dedicated to the advancement of aeronautics and space science. The NASA Scientific and Technical Information (STI) Program Office plays a key part in helping NASA maintain this important role.

The NASA STI Program Office is operated by Langley Research Center, the lead center for NASA's scientific and technical information. The NASA STI Program Office provides access to the NASA STI Database, the largest collection of aeronautical and space science STI in the world. The Program Office is also NASA's institutional mechanism for disseminating the results of its research and development activities. These results are published by NASA in the NASA STI Report Series, which includes the following report types:

- **TECHNICAL PUBLICATION.** Reports of completed research or a major significant phase of research that present the results of NASA programs and include extensive data or theoretical analysis. Includes compilations of significant scientific and technical data and information deemed to be of continuing reference value. NASA counterpart of peer-reviewed formal professional papers, but having less stringent limitations on manuscript length and extent of graphic presentations.
- **TECHNICAL MEMORANDUM.** Scientific and technical findings that are preliminary or of specialized interest, e.g., quick release reports, working papers, and bibliographies that contain minimal annotation. Does not contain extensive analysis.
- **CONTRACTOR REPORT.** Scientific and technical findings by NASA-sponsored contractors and grantees.

- **CONFERENCE PUBLICATION.** Collected papers from scientific and technical conferences, symposia, seminars, or other meetings sponsored or co-sponsored by NASA.
- **SPECIAL PUBLICATION.** Scientific, technical, or historical information from NASA programs, projects, and missions, often concerned with subjects having substantial public interest.
- **TECHNICAL TRANSLATION.** English-language translations of foreign scientific and technical material pertinent to NASA's mission.

Specialized services that complement the STI Program Office's diverse offerings include creating custom thesauri, building customized databases, organizing and publishing research results ... even providing videos.

For more information about the NASA STI Program Office, see the following:

- Access the NASA STI Program Home Page at <http://www.sti.nasa.gov>
- E-mail your question via the Internet to [help@sti.nasa.gov](mailto:help@sti.nasa.gov)
- Fax your question to the NASA STI Help Desk at (301) 621-0134
- Phone the NASA STI Help Desk at (301) 621-0390
- Write to:  
NASA STI Help Desk  
NASA Center for AeroSpace Information  
7121 Standard Drive  
Hanover, MD 21076-1320

NASA/TP-2005-213943



# The Effect of Basis Selection on Static and Random Acoustic Response Prediction Using a Nonlinear Modal Simulation

*Stephen A. Rizzi*  
*Langley Research Center, Hampton, Virginia*

*Adam Przekop*  
*National Institute of Aerospace, Hampton, Virginia*

National Aeronautics and  
Space Administration

Langley Research Center  
Hampton, Virginia 23681-2199

December 2005

The use of trademarks or names of manufacturers in the report is for accurate reporting and does not constitute an official endorsement, either expressed or implied, of such products or manufacturers by the National Aeronautics and Space Administration.

Available from:

NASA Center for AeroSpace Information (CASI)  
7121 Standard Drive  
Hanover, MD 21076-1320  
(301) 621-0390

National Technical Information Service (NTIS)  
5285 Port Royal Road  
Springfield, VA 22161-2171  
(703) 605-6000

## **ABSTRACT**

An investigation of the effect of basis selection on geometric nonlinear response prediction using a reduced-order nonlinear modal simulation is presented. The accuracy is dictated by the selection of the basis used to determine the nonlinear modal stiffness. The scope of this investigation is limited to structures which do not exhibit linear bending-membrane coupling, but do exhibit nonlinear bending-membrane coupling. This study considers a suite of available bases including bending modes only, bending and membrane modes, coupled bending and companion modes, and uncoupled bending and companion modes. Companion modes represent an alternative to membrane modes and capture some of the membrane behavior resulting from bending-membrane coupling. The nonlinear modal simulation presented is broadly applicable and is demonstrated for nonlinear quasi-static and random acoustic response of flat beam and plate structures with isotropic material properties. Reduced-order analysis predictions are compared with those made using a numerical simulation in physical degrees-of-freedom to quantify the error associated with the selected modal bases. Bending and membrane responses are separately presented to help differentiate the bases.

## **1. INTRODUCTION**

The design of advanced aerospace vehicle components capable of withstanding high vibroacoustic environments is hampered by a lack of accurate and computationally fast methods. Such methods are required in the design phase to quickly assess the impact of design changes on high-cycle fatigue life. Linear analysis methods are often inappropriate as structures may respond in a geometrically nonlinear fashion. Therefore, the use of a nonlinear analysis is required. Complicated structural geometries dictate the use of a finite element analysis (FEA). The traditional FEA employing numerical simulation in physical degrees-of-freedom (DoFs), however, is computationally intensive and considered impractical in design environments where rapid prototyping is needed. For stochastic response, the computational burden is exacerbated by the need to perform probabilistic analysis, such as Monte Carlo simulation [1, 2], which requires that multiple realizations of the response be computed to generate meaningful statistics. Therefore, alternative methods are sought which retain the level of accuracy required, yet are computationally efficient.

Reduced-order nonlinear finite element analysis methods gain their computational advantage over direct numerical simulation by transforming the equations of motion in physical DoFs to modal coordinates. Consequently, system size is significantly reduced and can be solved in a time efficient manner by means of numerical simulation or by an equivalent linearization approach, as dictated by the desired fidelity of the analysis. In the recent past, equivalent linearization procedures [3, 4] have been shown to be applicable [5, 6] to this class of problems, albeit in an approximate sense. This study focuses on reduced-order numerical integration analysis.

The problems of interest in this paper are those in which the structure responds to imposed loads in a geometrically nonlinear (large deflection) static and random fashion. This nonlinearity is due to bending-membrane coupling and gives rise to membrane stretching when out-of-plane loading is applied. Consideration of structures which exhibit linear bending-membrane coupling is outside the scope of this work. Structures which exhibit linear bending-membrane coupling include curved structures and non-symmetrically laminated composites with a non-zero coupling stiffness matrix  $[B]$ . In the recent past, a significant amount of research has been performed in reduced-order methods development that is applicable to the class of problems of interest. These methods may be viewed as being in one of two categories; those in which the nonlinear modal stiffness is directly evaluated from the nonlinear finite element stiffness matrix (so-called direct methods), and those in which the nonlinear modal stiffness is indirectly evaluated. Direct methods are typically implemented in special purpose finite element codes in which the nonlinear stiffness is known. The work by Mei et al [7] for flat configurations and the expansion of that approach for curved panels by Przekop et al [8, 9] are good examples of the direct method. In physical coordinates, the membrane displacements may be statically condensed into the bending displacements by neglecting in-plane inertia, and thus eliminate the need for membrane modes in the modal basis. This approach is sometimes referred to as “direct physical condensation” [10]. Alternatively, modal in-plane inertia may be neglected once the system of equations is transformed to modal coordinates, in an approach subsequently referred to as “direct modal condensation.” In this variation, the membrane behavior must still be represented in the basis.

For the analysis of complicated structures, commercial finite element codes are often required due to their support for a large number of element types. Unfortunately, the nonlinear stiffness is not typically available, making implementation of the direct method not possible. The only known implementation of a direct method into a commercial code is due to Bathe and Gracewski [11], in the ADINA finite element program. Indirect stiffness evaluation methods arose from the desire to implement reduced-order nonlinear analyses within the context of any commercial finite element analysis. Examples of indirect stiffness evaluation approaches may be found in the work of McEwan et al [12, 13] and Muravyov and Rizzi [14]. The approach taken by McEwan involves solution of a series of nonlinear static problems, typically through application of static forces with distributions corresponding to bending modes only. Following a modal coordinate transformation, the nonlinear modal stiffness is determined by curve fitting the modal force – displacement relation. Because the nonlinear static problem uses prescribed forces, the displacement response is influenced by the effect of membrane stiffness resulting from nonlinear bending-membrane coupling. The effect of membrane modes is thus implicitly condensed into the bending modes. This is advantageous in that explicit inclusion of membrane modes in the modal basis is eliminated. The implicit condensation of membrane modes however renders the approach unable to directly determine membrane displacements. Recently a post-processing procedure involving a mapping technique, called an “estimated expansion basis” [15], was developed to mitigate this problem. Nevertheless, the implicit condensation method is capable of producing only cubic nonlinear modal stiffness terms [15]. Its general applicability to non-planar structures, in which the effects of quadratic stiffness and membrane inertia may be significant, has yet to be explored.

By contrast, the approach undertaken by the authors solves a series of simple algebraic equations obtained from static nonlinear analyses using prescribed displacements obtained from a combination of basis vectors. For the problems under consideration, the low-frequency bending modes obtained from the linear eigenvalue problem are uncoupled from the high-frequency membrane modes. In past works by the authors [5, 14], the basis vectors were formed from only low-frequency bending modes. However, to more accurately represent the effect of nonlinear bending-membrane coupling, the membrane response must be explicitly represented through inclusion of some form of membrane response in the basis. Inclusion of membrane modes may be cumbersome because the task of identifying a particular high-frequency membrane mode

amongst a great number of computed modes is labor intensive. In recognition of that, Hollkamp et al [10, 15] and Mignolet et al [16] have developed “companion” or “dual” modes to help capture the effect of membrane response, without explicitly including membrane modes in the basis.

For both direct and indirect stiffness evaluation approaches, the accuracy of the solution depends on the selection of the modal basis, through which the nonlinear modal stiffness may be determined. If an insufficient basis is selected, then the predicted dynamic response of the reduced-order model may significantly differ from that of the full nonlinear model. Thus, there is always a need to assess the appropriateness of the selected basis via comparison of the predicted reduced-order response with something other than a reduced-order method, e.g. experimental data or numerical simulation in physical DoFs. Recent work compared various reduced-order approaches with experimental data [10]. In this study, comparisons are made with numerical simulation in physical DoFs to permit identical specification of boundary conditions.

This paper assesses the effect of basis selection on the response obtained from a nonlinear modal simulation, utilizing the authors’ indirect stiffness evaluation method. A suite of bases is considered including bending modes only, bending and membrane modes, coupled bending and companion modes, and uncoupled bending and companion modes. The effect of basis selection on the modal stiffness coefficients themselves is first investigated. Then, using these coefficients, the nonlinear quasi-static and random response of simple planar aluminum beam and plate structures under spatially uniform excitation is considered. These structures were selected to help keep the cost of the comparative physical DoFs simulation reasonable, yet retain the nonlinear bending-membrane coupling behavior of interest. The error associated with the modal basis selection is quantified for both the displacement and stress response. Bending and membrane responses are separately presented to help differentiate the bases.

## **2. NONLINEAR MODAL SIMULATION**

The nonlinear modal simulation analysis employed in this work consists of several parts. One or more methods, to be discussed, are first used to obtain a modal basis. Following a transformation of the nonlinear system to modal coordinates, the modal stiffness coefficients are evaluated and the resulting coupled system of equations is numerically integrated to obtain the

modal displacement time history. These are transformed back to physical coordinates for post-processing, including stress recovery.

## 2.1. MODAL COORDINATE TRANSFORMATION

The equations of motion of the nonlinear system in physical DoFs may be written as

$$\mathbf{M}\ddot{\mathbf{X}}(t) + \mathbf{C}\dot{\mathbf{X}}(t) + \mathbf{F}_{NL}(\mathbf{X}(t)) = \mathbf{F}(t) \quad (1)$$

where  $\mathbf{M}$  and  $\mathbf{C}$  are the mass and proportional damping matrices, respectively,  $\mathbf{X}$  is the displacement response vector and  $\mathbf{F}$  is the force excitation vector. As written, the nonlinear restoring force vector,  $\mathbf{F}_{NL}$ , contains the linear force  $\mathbf{K}\mathbf{X}$  and nonlinear forces, where  $\mathbf{K}$  is the linear stiffness.

A set of coupled modal equations with reduced DoFs is first obtained by applying the modal coordinate transformation  $\mathbf{X} = \mathbf{\Phi}\mathbf{q}$  to Equation (1), where  $\mathbf{q}$  is the vector of modal coordinates. The modal basis matrix  $\mathbf{\Phi}$  is typically formed from the eigenvectors obtained from Equation (1) using only the linear stiffness. For flat isotropic structures, these may include any combination of bending and membrane modes. In lieu of membrane modes, the modal basis may include “companions” related to the membrane response, as discussed in the next section. Generally, a small set ( $L$ ) of basis vectors are included giving

$$\tilde{\mathbf{M}}\ddot{\mathbf{q}}(t) + \tilde{\mathbf{C}}\dot{\mathbf{q}}(t) + \tilde{\mathbf{F}}_{NL}(q_1(t), q_2(t), \dots, q_L(t)) = \tilde{\mathbf{F}}(t) \quad (2)$$

where, for mass-normalized eigenvectors,

$$\begin{aligned} \tilde{\mathbf{M}} &= \mathbf{\Phi}^T \mathbf{M} \mathbf{\Phi} = [\mathbf{I}] \\ \tilde{\mathbf{C}} &= \mathbf{\Phi}^T \mathbf{C} \mathbf{\Phi} = [2\zeta_r \omega_r] \\ \tilde{\mathbf{F}}_{NL} &= \mathbf{\Phi}^T \mathbf{F}_{NL} \\ \tilde{\mathbf{F}} &= \mathbf{\Phi}^T \mathbf{F} \end{aligned} \quad (3)$$

and  $\omega_r$  are the undamped natural frequencies and  $\zeta_r$  are the viscous damping factors.

## 2.2. MODAL BASIS SELECTION

For the problems of interest in this paper, both bending and membrane behavior should be included in the basis selection since the large deflection nonlinearity couples their response. The basis vectors may be determined via several methods. Bases corresponding to the bending and membrane response may be determined through solution of the linear eigenvalue problem. Other basis vectors corresponding to the membrane response induced by bending-membrane coupling may be determined via alternative approaches, as discussed in Sec. 2.2.2. Lastly, while not the subject of this paper, basis vectors may also be determined via experiment or a hybrid scheme.

### 2.2.1 Linear Eigenvectors

Recall that for the problems of interest, the linear eigenvectors, obtained from Equation (1) using only the linear stiffness, are uncoupled and are either associated with low-frequency bending modes or high-frequency membrane modes. The selection of which bending modes to include depends on a number of factors including the excitation bandwidth, the spatial loading distribution, and even geometric and material properties. The selection of which membrane modes to include is less apparent than bending modes, as these high-frequency modes typically reside above the excitation bandwidth. Nevertheless, a reasonable starting point is to select the lowest membrane modes that are consistent with the spatial loading distribution and other physical properties. For example, for a uniform flat structure under uniform transverse loading, the membrane displacement will be anti-symmetric, so anti-symmetric membrane modes would be selected. Inclusion of both bending and membrane eigenvectors in the modal basis, either independently or in pairs, is subsequently referred to as the bending and membrane mode (BM) basis. Inclusion of only the bending eigenvectors will be referred to as the bending mode only (B) basis. In this study, the mass-normalized eigenvectors were obtained using MSC.NASTRAN normal modes analysis (solution 103).

### 2.2.2 Companion Basis Vectors

An alternative approach to using membrane modes is the use of so-called companion [10] or dual [16] modes. These modes are meant to represent the membrane behavior resulting from bending due to bending-membrane coupling. Previous authors utilized quasi-static approaches to determine the companion mode via nonlinear static analyses. For each companion mode,

Hollkamp et al [10] prescribed a displacement field corresponding to the bending mode of interest. Mignolet et al [16] applied two loadings, each having the distribution of a particular bending mode shape but with different magnitudes, to obtain the companion for that bending mode. In either case, the resulting modes contained only the membrane related behavior, but not the bending. The companion modes obtained need to be mass-normalized prior to their use.

A new method is now presented for computing the companion mode using a dynamic analysis. An initial stress-free, out-of-plane perturbation of the mesh is first introduced to couple the bending-membrane response. The magnitude of the perturbation is chosen to be very small such that a normal modes analysis yields virtually the same bending eigenvalues and eigenvectors as that of the flat structure. An engineering rationale for specifying the shape of the perturbation is not evident. It was found that the companion modes change with varying perturbation shapes. In this investigation, the shape was chosen to be that of the first bending mode. The bending and high frequency membrane components remained identical to that of the flat structure, regardless of the shape of the perturbation. The MSC.NASTRAN normal modes analysis was again used to compute the mass-normalized eigenvectors, which now contain both the bending and membrane behaviors, but at the natural frequencies of the original flat structure. Direct inclusion of these eigenvectors in the modal basis is subsequently referred to as the coupled bending and companion mode (CBC) basis.

A more consistent usage of companion modes, with respect to references [10, 16], is to separate the DoFs associated with the bending and membrane behaviors. In practice, since the bending behavior is unchanged, the original low-frequency bending modes are retained. The bending DoFs are set to zero in the newly obtained eigenvector to obtain the uncoupled dynamic companion. Since the uncoupled dynamic companion is essentially obtained by partitioning the mass-normalized CBC mode, it is no longer itself mass-normalized. Therefore, an additional step of mass-normalization is necessary. Inclusion of both the original bending and uncoupled dynamic companion modes in the modal basis, independently or in pairs, is subsequently referred to as the uncoupled bending and companion mode (UBC) basis.

### 2.2.3 Comparison of Membrane and Companion Modes

Consider a clamped-clamped aluminum beam measuring 18-in. x 1-in. x 0.09-in ( $l \times w \times h$ ) with the following material properties:

$$E = 10.6 \times 10^6 \text{ psi}, \quad G = 4.0 \times 10^6 \text{ psi}, \quad \rho = 2.588 \times 10^{-4} \frac{\text{lb}_f \text{-s}^2}{\text{in}^4}$$

The beam was modeled in MSC.NASTRAN using 144 CBEAM elements. At the clamped ends, all DoFs are constrained. For the uniformly distributed loadings to follow, the first six symmetric bending modes (eigenvectors 1, 3, 7, 10, 14 and 19) at natural frequencies of 58, 312, 770, 1431, 2293 and 3354 Hz, respectively, were selected. The first six anti-symmetric membrane modes (eigenvectors 46, 81, 115, 153, 221 and 231) are at natural frequencies of 11.2, 22.5, 33.7, 44.9, 56.1 and 67.3 kHz, respectively. The first four of these are plotted in Figure 1 – Figure 4. Also shown are the static companion modes obtained by Mignolet’s approach [16] and the dynamic companion modes obtained by the method outlined above. It is clear that both static and dynamic companion modes significantly differ in shape relative to the membrane mode. The effect of their inclusion in the modal basis on the stiffness coefficients is next considered.

### 2.3. INDIRECT STIFFNESS EVALUATION METHOD

The indirect stiffness evaluation method previously developed [14, 16] was used in this study. To summarize, the nonlinear force vector in Equation (2) may be written in the form

$$\tilde{F}_{NL}(q_1, q_2, \dots, q_L) = \sum_{j=1}^L d_j^r q_j + \sum_{j=1}^L \sum_{k=j}^L a_{jk}^r q_j q_k + \sum_{j=1}^L \sum_{k=j}^L \sum_{l=k}^L b_{jkl}^r q_j q_k q_l \quad r = 1, 2, \dots, L \quad (4)$$

reducing the problem of determining the nonlinear stiffness from one in which a large set of simultaneous nonlinear equations must be solved to one involving simple algebraic relations. The linear, quadratic, and cubic nonlinear modal stiffness coefficients are written as  $d_j$ ,  $a_{jk}$  and  $b_{jkl}$ , respectively.

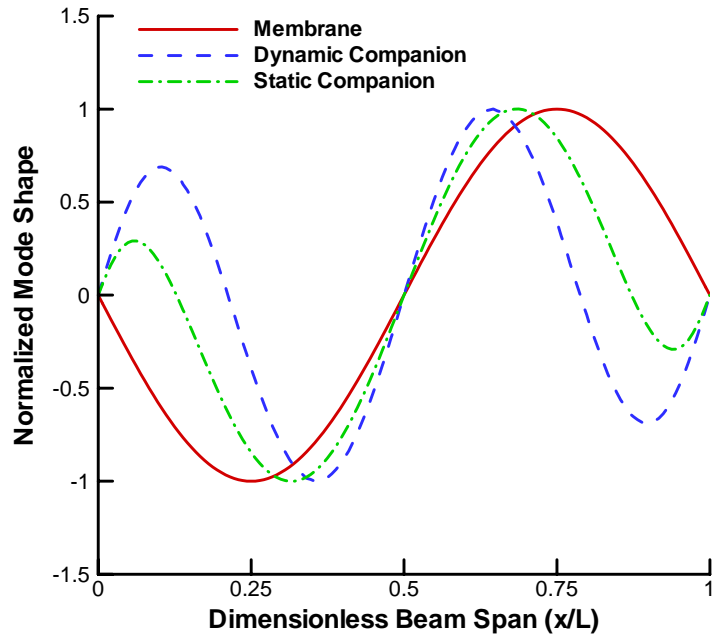


Figure 1: First anti-symmetric membrane and companion modes.

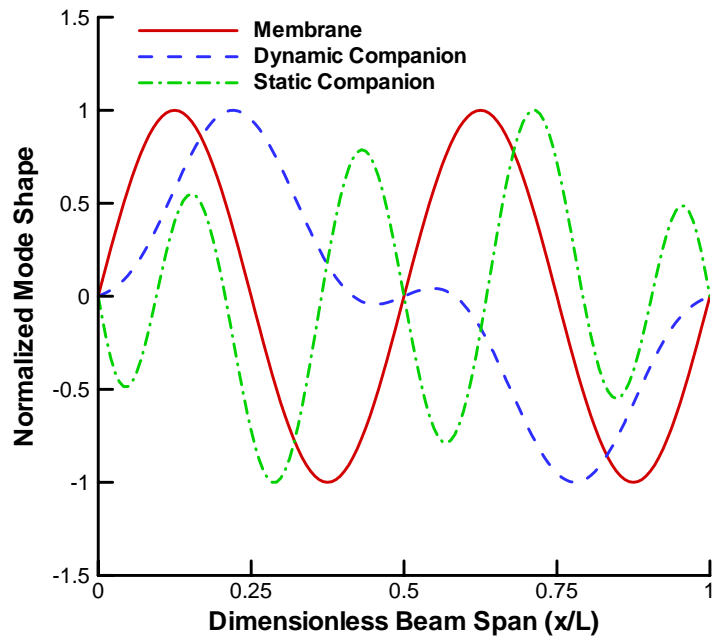


Figure 2: Second anti-symmetric membrane and companion modes.

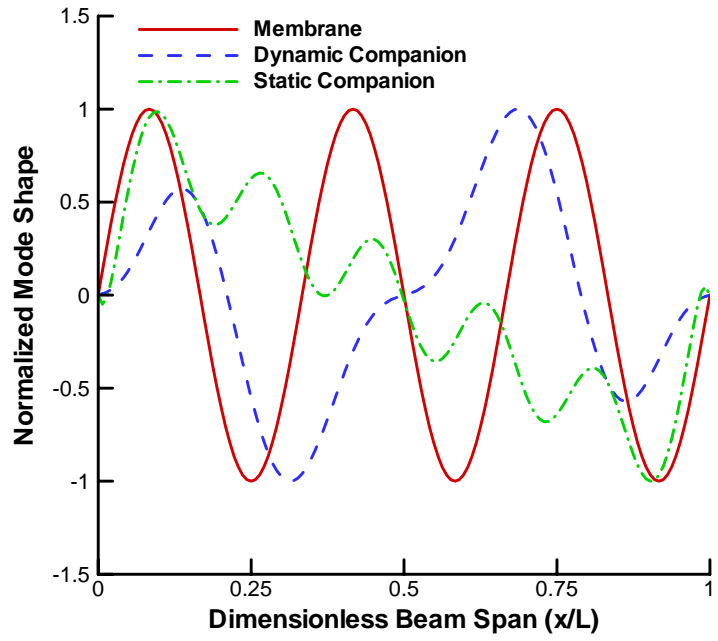


Figure 3: Third anti-symmetric membrane and companion modes.

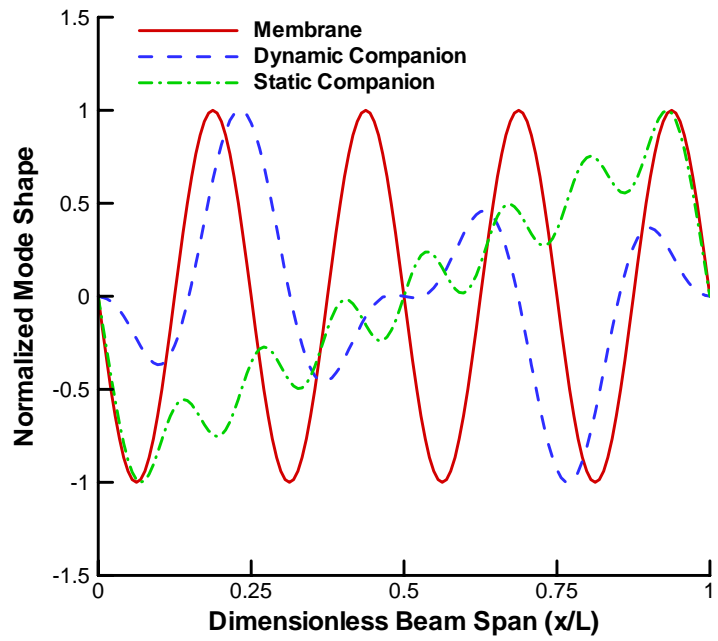


Figure 4: Fourth anti-symmetric membrane and companion modes.

For the prescribed *static* displacement fields [16]

$$\mathbf{X}_{c1} = +\phi_1 q_1 \quad \mathbf{X}_{c2} = -\phi_1 q_1 \quad \mathbf{X}_{c3} = +\phi_1 \hat{q}_1 \quad (5)$$

the nonlinear forces evaluated using the MSC.NASTRAN nonlinear static solution (solution 106) are given as

$$\begin{aligned} \tilde{\mathbf{F}}_{NL_1} &= \mathbf{\Phi}^T \mathbf{F}_{NL} (+\phi_1 q_1) = +[d_1^r] q_1 + [a_{11}^r] q_1 q_1 + [b_{111}^r] q_1 q_1 q_1 \\ \tilde{\mathbf{F}}_{NL_2} &= \mathbf{\Phi}^T \mathbf{F}_{NL} (-\phi_1 q_1) = -[d_1^r] q_1 + [a_{11}^r] q_1 q_1 - [b_{111}^r] q_1 q_1 q_1 \\ \tilde{\mathbf{F}}_{NL_3} &= \mathbf{\Phi}^T \mathbf{F}_{NL} (+\phi_1 \hat{q}_1) = +[d_1^r] \hat{q}_1 + [a_{11}^r] \hat{q}_1 \hat{q}_1 - [b_{111}^r] \hat{q}_1 \hat{q}_1 \hat{q}_1 \end{aligned} \quad (6)$$

The first two of Equation (6) are used to evaluate  $[a_{11}^r]$ . The first and the third of Equation (6) are then used to determine  $[d_1^r]$  and  $[b_{111}^r]$ . It should be noted that the specified modal displacements in Equation (5) are single scalar quantities since the analysis is static. These modal displacements are specified such that the magnitude of the prescribed physical displacement field  $\mathbf{X}_c$  is physically meaningful. It has been shown that the stiffness coefficients obtained via this approach are not sensitive to the particular value of modal displacement specified [14]. The last of Equation (5) are obtained by specifying a scaled modal displacement such that  $\hat{q} = \alpha q$ . It was found in the course of this work that the stiffness coefficients obtained were also insensitive to the particular value of  $\alpha$  used. In this paper, values of  $q = 7 \times 10^{-5}$  and  $\alpha = 1.25$  were used for all modes in the basis.

This procedure for evaluating the linear stiffness coefficients  $[d_1^r]$  is advantageous over the earlier implementation [14] using the MSC.NASTRAN linear static solution (solution 101), as the linear solution does not include in-plane displacements, and therefore is not capable of handling thermal loads. The remaining nonlinear coefficients are evaluated through an additional series of nonlinear static solutions, as described in [14].

### 2.3.1 Comparison of Modal Stiffness Coefficients

For the clamped-clamped beam structure previously considered, the effect of including a particular set of modes in the modal basis is shown in Table 1 – Table 5. Table 1 shows the

diagonal terms of the linear stiffness coefficients for a set consisting of the first six symmetric bending modes ( $d_1^1 - d_6^6$ ) plus up to six membrane or companion modes ( $d_7^7 - d_{12}^{12}$ ). For each basis, the first six linear stiffness coefficients are equal to the eigenvalues of the selected bending modes. For the BM basis, the second six linear stiffness coefficients correspond to the eigenvalues of the selected membrane modes. The CBC basis lacks the second set of six coefficients as only six modes are included in this basis, i.e. six coupled bending and companion modes. It is interesting to note that the stiffness coefficients for companion modes of both UBC bases differ from each other and from the membrane. Thus, there is no physical meaning to the linear stiffness coefficients  $d_7^7 - d_{10}^{10}$  associated with the companion modes for the UBC bases. Further, although comparable in magnitude to the membrane modes, the stiffness coefficients for companion modes of both UBC bases do not increase monotonically. For the CBC basis and both UBC bases, the off-diagonal terms are non-zero (not shown), indicating coupling of the linear stiffness where none should exist.

Table 1: Diagonal terms of beam linear stiffness obtained using five different modal bases. Shaded cells indicate bending eigenvalues.

	B	BM	CBC	UBC	UBC <sup>[16]</sup> (static)
$d_1^1$	1.318E+05	1.318E+05	1.318E+05	1.318E+05	1.318E+05
$d_2^2$	3.845E+06	3.845E+06	3.845E+06	3.845E+06	3.845E+06
$d_3^3$	2.341E+07	2.341E+07	2.341E+07	2.341E+07	2.341E+07
$d_4^4$	8.080E+07	8.080E+07	8.080E+07	8.080E+07	8.080E+07
$d_5^5$	2.075E+08	2.075E+08	2.075E+08	2.075E+08	2.075E+08
$d_6^6$	4.442E+08	4.442E+08	4.442E+08	4.442E+08	4.442E+08
$d_7^7$	N/A	4.990E+09	N/A	7.090E+10	1.487E+10
$d_8^8$	N/A	1.995E+10	N/A	7.621E+10	7.520E+10
$d_9^9$	N/A	4.485E+10	N/A	2.587E+09	5.846E+10
$d_{10}^{10}$	N/A	7.965E+10	N/A	2.057E+10	7.803E+10
$d_{11}^{11}$	N/A	1.243E+11	N/A	N/A	N/A
$d_{12}^{12}$	N/A	1.786E+11	N/A	N/A	N/A

Unlike direct physical and direct modal condensation, or the implicit condensation in McEwan's indirect approach, the effect of quadratic stiffness in the present stiffness evaluation approach is

not incorporated in the cubic stiffness, and must therefore be explicitly represented as indicated in Equation (4). Diagonal terms for the quadratic stiffness coefficients are shown in Table 2. The diagonal terms are expected to be zero for this flat structure, and essentially are for the B and BM bases. However, the CBC basis indicates significant coefficients for the first six modes ( $a_{11}^1 - a_{66}^6$ ). Stiffness coefficients for the companion modes of both UBC bases ( $a_{77}^7 - a_{10\ 10}^{10}$ ) are also significant, although their effect on the response is likely small for out-of-plane loadings. Interestingly, while the presence of anti-symmetric companion modes introduces significant diagonal terms for the CBC and UBC bases, the presence of anti-symmetric membrane modes does not affect the diagonal terms for the BM basis. The off-diagonal terms corresponding to the first (1<sup>st</sup> symmetric bending) and seventh (1<sup>st</sup> membrane or companion) modal equations are shown in Table 3, and indicate a coupling between modes for both UBC bases and the BM basis.

Table 2: Diagonal terms of beam quadratic stiffness obtained using five different modal bases.

	B	BM	CBC	UBC	UBC <sup>[16]</sup> (static)
$a_{11}^1 q_1$	-6.001E-11	-6.653E-11	6.937E+01	-3.673E-11	-1.737E-10
$a_{22}^2 q_2$	4.044E-10	1.028E-10	-1.474E+03	1.874E-12	4.471E-10
$a_{33}^3 q_3$	-1.400E-09	1.061E-09	2.701E+03	-5.210E-10	7.226E-09
$a_{44}^4 q_4$	-2.658E-09	-1.834E-09	3.879E+03	2.047E-09	-1.192E-07
$a_{55}^5 q_5$	7.535E-09	-6.914E-09	-5.006E+03	7.684E-10	5.356E-09
$a_{66}^6 q_6$	-3.101E-08	-2.980E-08	-6.295E+03	-4.212E-08	-2.676E-08
$a_{77}^7 q_7$	N/A	8.864E-06	N/A	-7.245E-01	6.642E+00
$a_{88}^8 q_8$	N/A	-4.808E-05	N/A	1.767E+00	1.570E+01
$a_{99}^9 q_9$	N/A	-4.976E-05	N/A	-5.094E-01	-7.283E+02
$a_{10\ 10}^{10} q_{10}$	N/A	-1.408E-04	N/A	-5.227E-01	-4.782E+03
$a_{11\ 11}^{11} q_{11}$	N/A	-4.697E-05	N/A	N/A	N/A
$a_{12\ 12}^{12} q_{12}$	N/A	5.307E-04	N/A	N/A	N/A

Relationships between quadratic modal stiffness coefficients were previously found in [14] and are given by

$$\begin{aligned} a_{17}^1 &= 2a_{11}^7 \\ 2a_{77}^1 &= a_{17}^7 \end{aligned} \quad (7)$$

Equation (7) should be satisfied for only the *significant* nonlinear coefficients. For the quadratic terms presented in Table 3, the BM basis satisfies the first of Equation (7). For both UBC bases, however, the significant terms do not satisfy the first of Equation (7). The second of Equation (7) is not satisfied for any basis because these terms are not significant.

Table 3: Selected off-diagonal quadratic stiffness terms obtained using five modal bases.

	B	BM	CBC	UBC	UBC <sup>[16]</sup> (static)
$a_{11}^1 q_1$	-6.001E-11	-6.653E-11	6.937E+01	-3.673E-11	-1.737E-10
$a_{17}^1 q_1$	N/A	<b>-2.320E+05</b>	N/A	<b>4.625E+01</b>	<b>-2.398E+01</b>
$a_{77}^1 q_7$	N/A	-1.118E-06	N/A	3.312E-15	3.608E-15
$a_{11}^7 q_1$	N/A	<b>-1.160E+05</b>	N/A	<b>7.119E+10</b>	<b>-8.107E+10</b>
$a_{17}^7 q_1$	N/A	-3.946E-01	N/A	5.389E+01	3.757E-01
$a_{77}^7 q_7$	N/A	8.864E-06	N/A	-7.245E-01	6.642E+00

Table 4 shows the diagonal terms of the cubic stiffness coefficients for the same modal bases as above. For each basis, all coefficients corresponding to the bending modes (1-6) are identical. Like the quadratic stiffness, coefficients corresponding to the companion modes of both UBC bases are large relative to those corresponding to the membrane modes of the BM basis. Selected off-diagonal stiffness coefficients are shown in Table 5. The most significant difference between the non-zero stiffness terms for the BM and UBC bases is that the  $b_{111}^7$  and the  $b_{777}^7$  terms are significant for the UBC bases and not for the BM basis. Conversely, the  $b_{177}^1$  term is significant for the BM basis but not for either UBC basis.

Relationships between cubic modal stiffness coefficients were previously found in [14] and are given by

$$\begin{aligned}
 b_{177}^1 &= b_{117}^7 \\
 3b_{777}^1 &= b_{177}^7 \cdot \\
 3b_{111}^7 &= b_{117}^1
 \end{aligned} \tag{8}$$

Like the quadratic terms, Equation (8) should be preserved for only the *significant* nonlinear cubic coefficients. For the cubic terms presented in Table 5, the BM basis approximately

satisfies the first of Equation (8). For both UBC bases, however, neither the first nor the third of Equation (8) are satisfied since terms on only one side of the equation are significant.

Table 4: Diagonal terms of beam cubic stiffness obtained using five different modal bases.

	B	BM	CBC	UBC	UBC <sup>[16]</sup> (static)
$b_{111}^1 q_1^2$	5.067E+02	5.067E+02	5.067E+02	5.067E+02	5.067E+02
$b_{222}^2 q_2^2$	3.626E+04	3.626E+04	3.626E+04	3.626E+04	3.626E+04
$b_{333}^3 q_3^2$	2.507E+05	2.507E+05	2.507E+05	2.507E+05	2.507E+05
$b_{444}^4 q_4^2$	9.124E+05	9.124E+05	9.124E+05	9.124E+05	9.124E+05
$b_{555}^5 q_5^2$	2.410E+06	2.410E+06	2.410E+06	2.410E+06	2.410E+06
$b_{666}^6 q_6^2$	5.248E+06	5.248E+06	5.248E+06	5.248E+06	5.248E+06
$b_{777}^7 q_7^2$	N/A	-4.897E-05	N/A	1.872E+02	-2.340E+02
$b_{888}^8 q_8^2$	N/A	3.534E-04	N/A	-3.522E+00	-1.121E+03
$b_{999}^9 q_9^2$	N/A	-3.199E-05	N/A	4.009E+01	1.121E+04
$b_{10\ 10\ 10}^{10} q_{10}^2$	N/A	5.931E-07	N/A	-1.499E+01	-9.658E+04
$b_{11\ 11\ 11}^{11} q_{11}^2$	N/A	2.756E-03	N/A	N/A	N/A
$b_{12\ 12\ 12}^{12} q_{12}^2$	N/A	-7.361E-03	N/A	N/A	N/A

Table 5: Selected off-diagonal cubic stiffness terms obtained using five different modal bases.

	B	BM	CBC	UBC	UBC <sup>[16]</sup> (static)
$b_{111}^1 q_1^2$	5.067E+02	5.067E+02	5.067E+02	5.067E+02	5.067E+02
$b_{117}^1 q_1 q_7$	N/A	-2.177E-06	N/A	-3.244E-11	2.418E-09
$b_{177}^1 q_1 q_7$	N/A	<b>-1.174E+03</b>	N/A	-2.829E-06	9.352E-07
$b_{777}^1 q_7^2$	N/A	-6.761E-07	N/A	2.310E-14	9.921E-15
$b_{111}^7 q_1^2$	N/A	7.559E-02	N/A	<b>5.522E+03</b>	<b>4.472E+04</b>
$b_{117}^7 q_1 q_7$	N/A	<b>-9.437E+02</b>	N/A	<b>8.816E+03</b>	<b>-3.782E+03</b>
$b_{177}^7 q_1 q_7$	N/A	-3.496E-01	N/A	5.390E-01	1.671E+00
$b_{777}^7 q_7^2$	N/A	-4.897E-05	N/A	<b>1.872E+02</b>	<b>-2.340E+02</b>

Further discussion regarding the choice of basis on the response prediction is reserved until Section 3.

## 2.4. NUMERICAL INTEGRATION AND ELEMENT STRESS RECOVERY

Having the nonlinear force vector in Equation (4) fully defined, the coupled modal nonlinear equations of motion in Equation (2) may be solved. An equivalent linearization approach was presented in [5] to solve the system in an approximate manner. A more accurate approach utilized in this paper numerically integrates Equation (2) using a fourth-order Runge-Kutta method [17]. The resulting modal displacement time histories are transformed back to physical coordinates using the inverse modal transformation.

Element stresses are recovered by post-processing the nodal physical DoFs directly within the finite element program. Since the stress post-processor of the finite element program is used, the stress calculation is identical to what would have been performed via a standard finite element analysis in physical DoFs. For a particular output time step, the element physical DoFs, obtained via the nonlinear modal simulation method, are applied to each element node as prescribed displacement fields in the MSC.NASTRAN nonlinear static solution and the element stresses are calculated. By repeating this operation for each output time step, the stress time history is determined.

## 3. NONLINEAR STATIC AND RANDOM ACOUSTIC RESPONSE OF A BEAM

The effect of modal basis selection on the nonlinear response is next considered for the same beam structure previously examined. It should be noted that the nonlinear modal simulation approach considered herein is applicable to arbitrary spatial and temporal loading distributions. Since the problems of interest originate from uniform acoustic loadings, the cases selected are limited to structures exposed to spatially uniform loadings. Therefore, while the calculation of nonlinear stiffness coefficients as described above is independent of the loading, conclusions drawn about the modal basis selection, specifically the choice of which modes to include for a particular basis type, are load-specific. The merits of one basis type (B, BM, CBC and UBC) versus another, however, can be assessed independent of the loading distribution. For the uniform spatial distribution considered, two temporal variations are considered; a quasi-static loading and a band-limited random acoustic loading. Results from the nonlinear modal simulation are compared with those obtained via numerical simulation in physical coordinates.

### 3.1. NUMERICAL SIMULATION IN PHYSICAL COORDINATES

Numerical simulation analyses in physical coordinates serves as the basis for comparison of results from nonlinear modal simulation analyses. The finite element program ABAQUS (version 6.4) was used to generate nonlinear displacement and stress time histories. The double precision explicit integration scheme with an adaptive time integration step (referred to as “element by element” in ABAQUS) was utilized for all analyses. The ABAQUS model consisted of 144 B21 elements. The choice of ABAQUS explicit analysis over alternative analysis methods, e.g. MSC.NASTRAN nonlinear transient solution (solution 129), was made based on its superior ability to simulate very long response histories. This choice introduced an inconsistency of element formulations used between the nonlinear modal and physical simulations. However, previous results (not shown) from a nonlinear static analysis in physical DoFs using MSC.NASTRAN (solution 106) and ABAQUS were nearly identical, indicating no significant difference between the different element formulations used.

### 3.2. QUASI-STATIC RESPONSE

In the limit of including all linear eigenvectors (the full set of BM modes) in the basis, results found using nonlinear modal simulation should be identical to those obtained via numerical simulation in physical coordinates because there is no modal truncation. The first purpose of the quasi-static response prediction is to investigate the effect of modal truncation. The second purpose is to investigate the spatial characteristics of results produced using each modal basis. Because the quasi-static response is considered, dynamic effects due to the modal mass and damping are not significant. Therefore, only the modal stiffness coefficients dictate the accuracy of the solution for a particular basis. Further, as these coefficients are the same for the quasi-static and subsequent dynamic analyses, the quasi-static analysis provides a benchmark against which the dynamic results may be judged.

While it is possible to set the modal accelerations and velocities to zero in Equation (2) and solve for the modal displacements via Newton-Raphson (as per [14]), the more direct approach utilized here applies a quasi-static loading and numerically integrates to obtain the modal displacements. Once transformed, the physical displacements and stresses obtained from the reduced-order

analysis are compared with those obtained from a nonlinear simulation in physical DoFs with the same quasi-static loading.

### 3.2.1 Load Generation and Stress Post-Processing

A uniformly distributed quasi-static pressure loading was applied to the beam to obtain the quasi-static response. The loading time history ramped from zero magnitude at time zero to its maximum level at 1.6384s, following which 0.5s of constant loading was applied. The response was obtained at 2.1384s, after the decay of any transient behavior.

The bending and membrane stress components were separated by averaging the upper and lower surface stresses to obtain the membrane component, and then subtracting that from the surface stress to obtain the bending component. This separation allowed greater insight into the effect of the various modal bases on the stress response.

### 3.2.2 Results

The effect of modal truncation was first considered. Three BM modal bases were used; a 4-mode basis consisting of the first two symmetric bending modes and first two anti-symmetric membrane modes (2+2), an 8-mode basis consisting of the first four symmetric bending modes and first four anti-symmetric membrane modes (4+4), and a 12-mode basis consisting of the first six symmetric bending modes and first six anti-symmetric membrane modes (6+6). Displacement results are presented at the  $\frac{1}{4}$  span (4.5-in. from the clamped end), and element stresses near the  $\frac{1}{4}$  span (4.4375-in. from the clamped end). These locations will help to elucidate the benefits and liabilities of the various modal bases under severe conditions as the membrane stress component is more significant there relative to the bending stress component than at other locations along the length, e.g., the clamped end or mid-span.

The transverse displacement response error is shown in Figure 5 for a range of loadings. Results shown in this and in the subsequent three figures are relative to the physical DoFs solution from the ABAQUS explicit analysis, i.e.,

$$\% \text{ Error} = \left( \frac{\text{Physical} - \text{Reduced Order}}{\text{Physical}} \right) \times 100 . \quad (9)$$

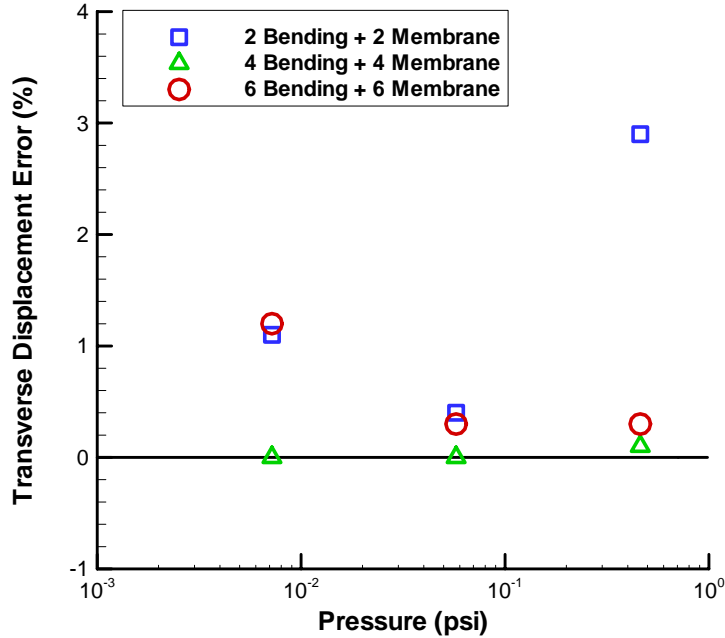


Figure 5: Transverse displacement error at beam  $\frac{1}{4}$  span for three BM bases.

It is seen that all bases except for 2+2 agree very well with the physical DoFs solution and asymptote to a small error. Since the subsequent random analysis in physical DoFs could only be performed using the ABAQUS explicit solution, the same solution was used here for consistency. Note that if the MSC.NASTRAN nonlinear static solution was used instead of the ABAQUS explicit analysis, a different set of small errors would be obtained. For example, for the 6+6 basis, at the highest level of 0.4608 psi, the error would be -0.07% using MSC.NASTRAN instead of +0.3%. Since the error is very small, Figure 5 should not be misinterpreted to indicate that the 4+4 basis is superior to the 6+6 basis at the highest loading level. Rather, the error in the 4+4 and 6+6 reduced-order analyses falls into an error band that is insignificant, regardless of the physical DoFs solution used for comparison.

The membrane displacement response error is shown in Figure 6. Here the 2+2 basis substantially under-predicts the response across the loading range, the 4+4 basis slightly over-predicts, and the 6+6 basis compares well across the range. The errors in bending and membrane stress components are shown in Figure 7 and Figure 8, respectively. In both cases, the 6+6 basis compares the most favorably across the loading range. The above results show that it is possible to achieve highly accurate displacement and stress response predictions using a truncated BM basis.

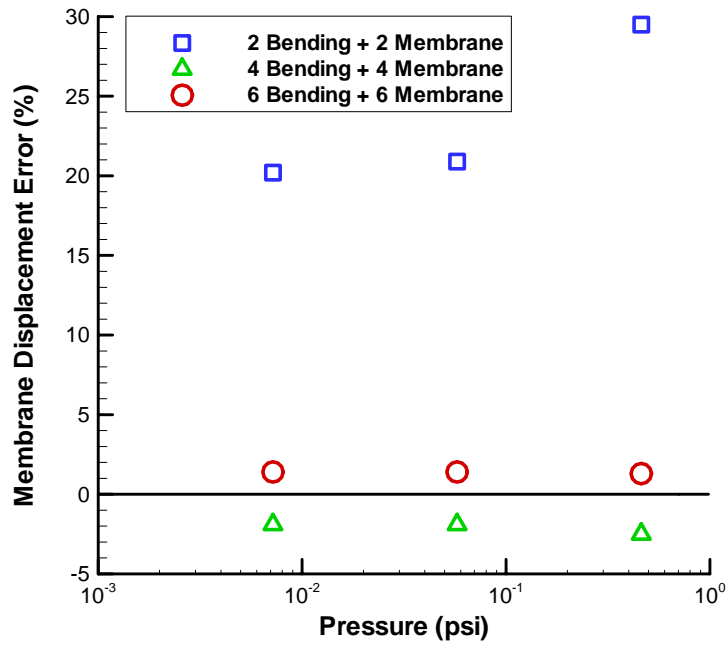


Figure 6: Membrane displacement error at beam  $\frac{1}{4}$  span for three BM bases.

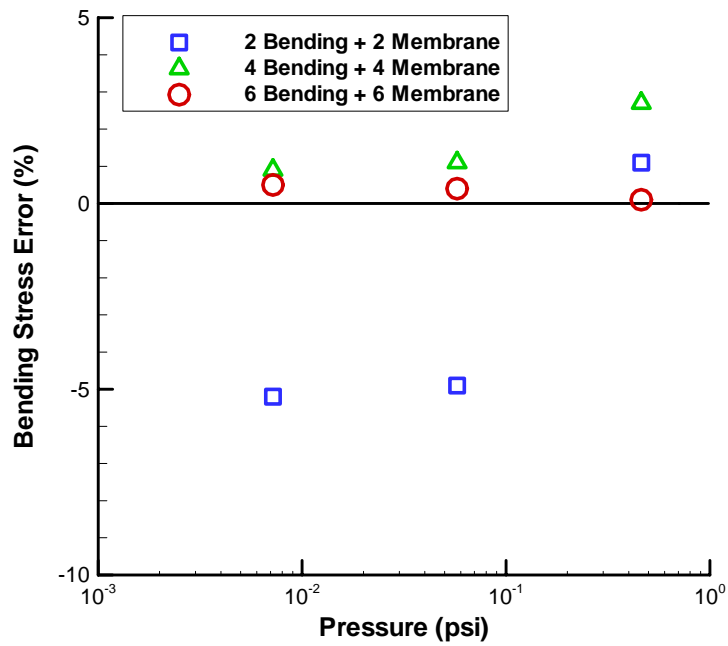


Figure 7: Bending stress error at beam  $\frac{1}{4}$  span for three BM bases.

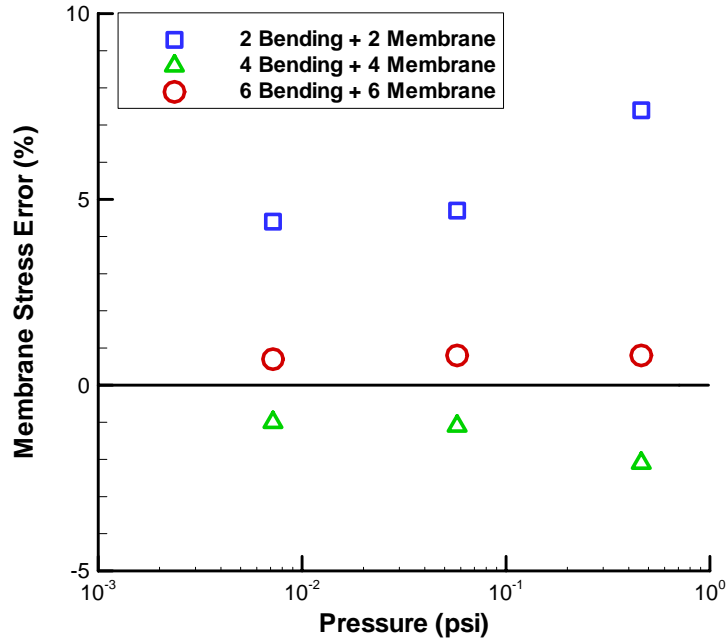


Figure 8: Membrane stress error at beam  $\frac{1}{4}$  span for three BM bases.

Next considered are the effects of different modal basis variants having a comparable number of included modes. The following modal bases were considered; the first six symmetric bending and first six anti-symmetric membrane modes (BM 6+6), the first six symmetric bending modes (B 6), the first six coupled bending-companion modes (CBC 6), and the dynamic version of UBC having the first six symmetric bending modes and first four companion modes (6+4). A numerical instability for both UBC bases was encountered, limiting the number of companion modes for a particular excitation level. Radu et al [18] attributed this problem to the high frequency content of the companion modes. However, since the problem was not observed for the BM basis having comparable frequency content, a more likely reason has to do with the high degree of coupling between some bending and companion modes, as previously discussed. A static condensation in modal coordinates was proposed and demonstrated to mitigate this behavior [18], although no attempt was made to implement this scheme in the present work. The instability was severe enough, however, that results for the UBC static basis could not be obtained for the quasi-static loading case. For this reason, only the (6+4) UBC dynamic basis was considered.

A single loading level (0.0576 psi) was applied and results are presented at locations across the beam semi-span to show how accuracy varies with location. Transverse displacements for each

modal basis are shown in Figure 9. The BM and UBC bases compare very well with the physical DoFs solution, while the B and CBC somewhat under-predict the response. By comparison, only the BM basis compares well with the membrane displacements shown in Figure 10. The bending-only basis B is incapable of predicting any membrane displacement, while the CBC basis correctly predicts the shape, but significantly under-predicts the magnitude. The UBC basis both over-predicts the magnitude and incorrectly predicts the shape.

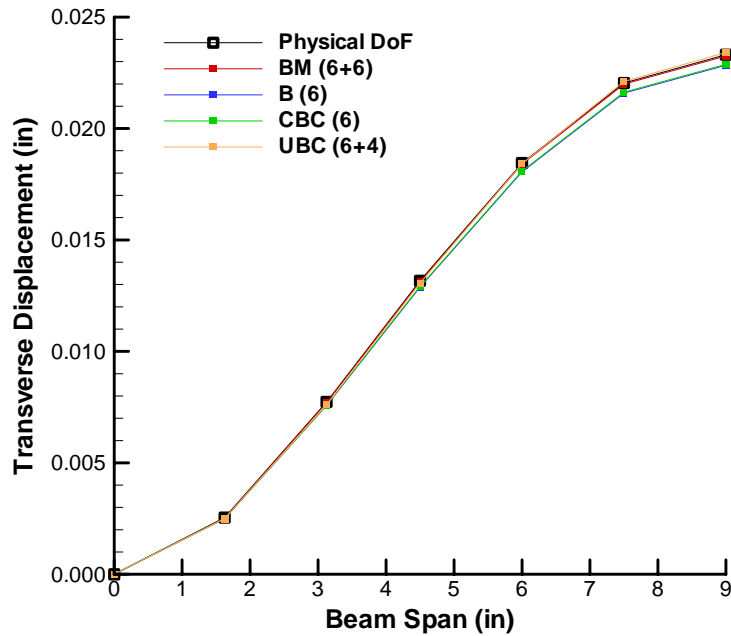


Figure 9: Quasi-static transverse displacements along beam semi-span for 4 modal bases.

The bending and membrane stress behaviors are shown in Figure 11 and Figure 12, respectively. Bending stress results from all bases compare well with the physical DoFs solution. The nearly constant membrane stress is accurately captured by only the BM basis. The other bases predict incorrect magnitudes and spatial distributions. With regard to the bending-only basis, the membrane stress arises from the bending-membrane coupling in the stress recovery calculation, even though this basis predicts a zero membrane displacement. The fact that there are several points along the beam where membrane stress results from the B, CBC and UBC agree with the physical DoFs solution highlights the need to consider a number of spatial locations in assessing the accuracy of the modal basis. Note that only the BM basis accurately predicts bending and membrane displacement and stress response at all span-wise locations.

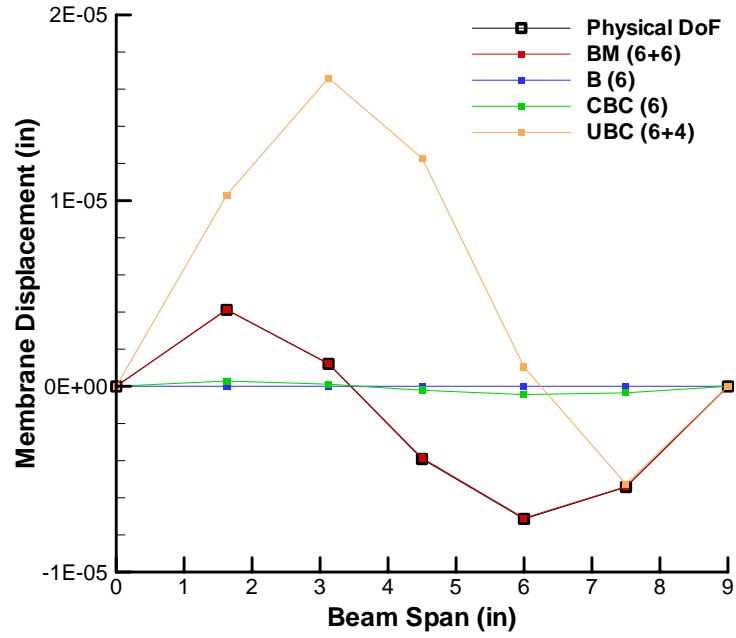


Figure 10: Quasi-static membrane displacements along beam semi-span for 4 modal bases.

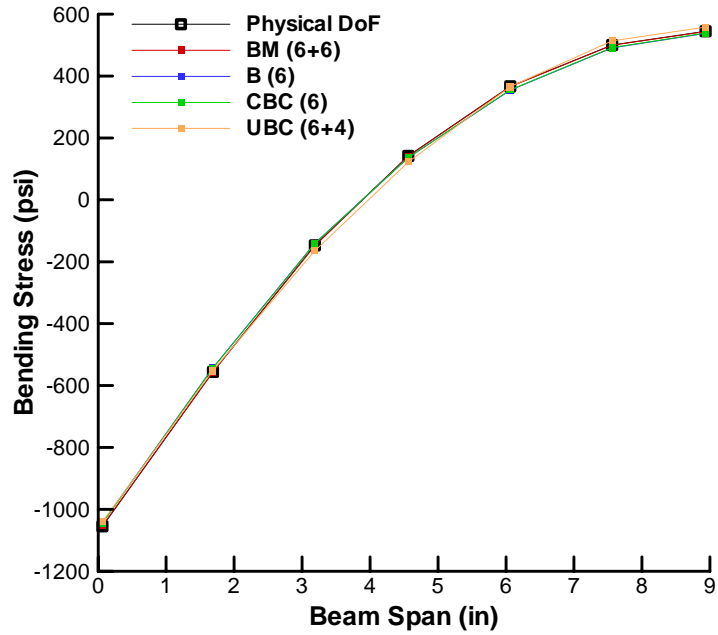


Figure 11: Quasi-static bending stress along beam semi-span for 4 modal bases.

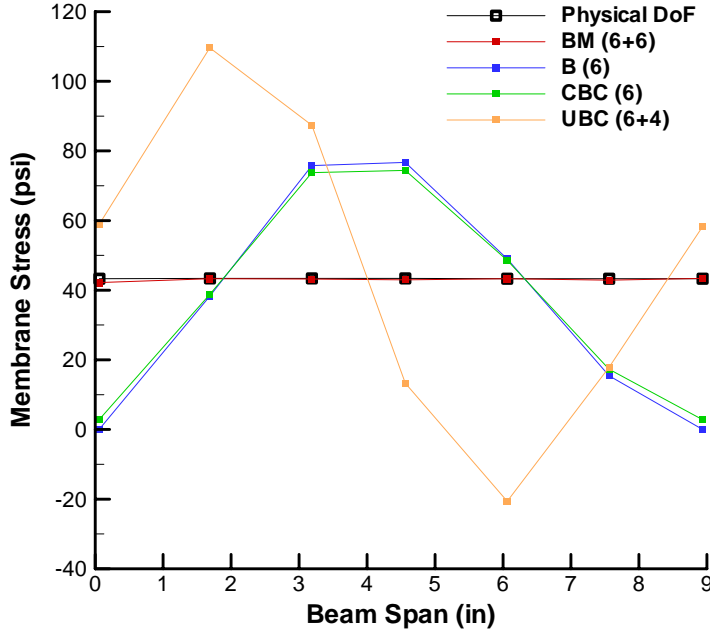


Figure 12: Quasi-static membrane stress along beam semi-span for 4 modal bases.

A compact measure of an error along the span of the beam may be found from

$$\% \text{ Error} = \left[ \frac{1}{N} \sum_{i=1}^N \sqrt{\frac{(\text{Physical}_i - \text{Reduced Order}_i)^2}{\text{Physical}_i^2}} \right] \times 100 \quad (10)$$

where  $N$  is a number of points along the beam span used for the estimation. Figure 13 and Figure 14 present the transverse and membrane displacement errors, respectively. It is seen that BM basis provide the best reduced-order approximation through the entire range of excitation levels studied. From Figure 14 it can be also concluded that while the CBC basis outperforms the UBC basis, both incur unacceptably large errors.

Figure 15 and Figure 16 present the bending and membrane stress errors, respectively. For the bending stress, the superiority of the BM basis is most evident at the highest loading. For the membrane stress, only the BM basis achieves errors less than 5%, while the B, CBC and UBC bases incur unacceptably large errors.

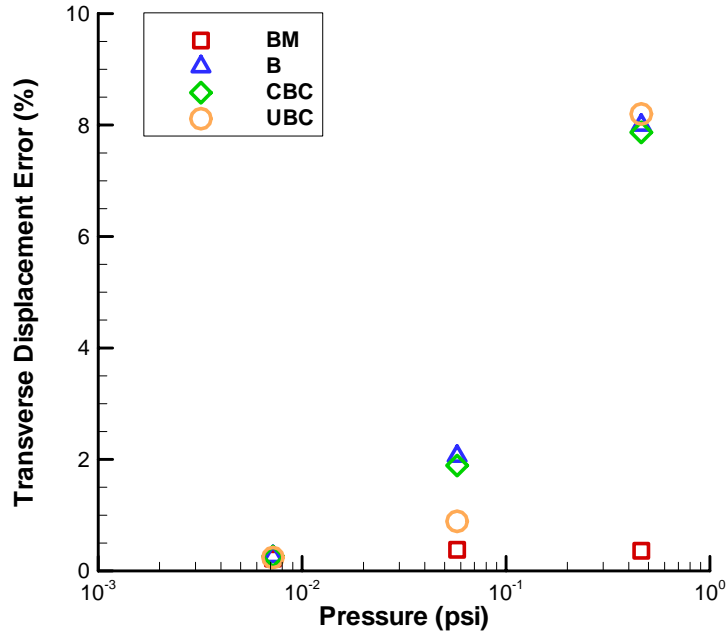


Figure 13: Quasi-static transverse displacement error integrated along the beam span.

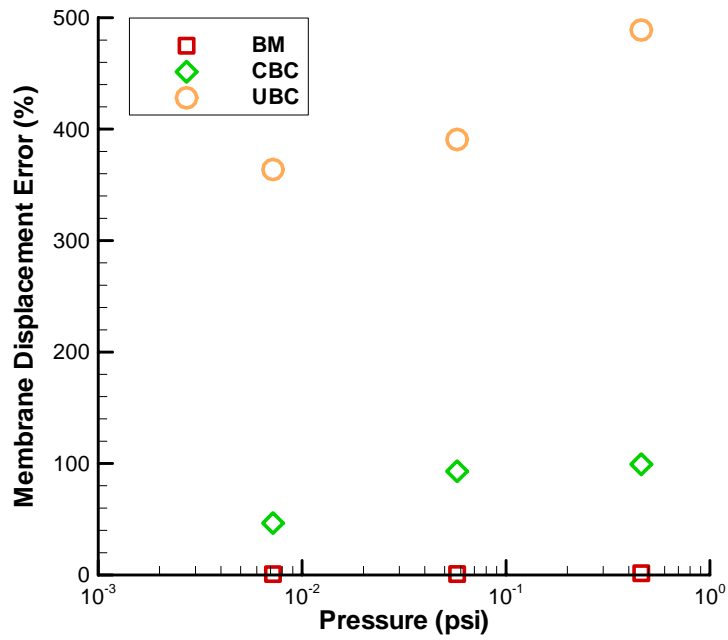


Figure 14: Quasi-static membrane displacement error integrated along the beam span.

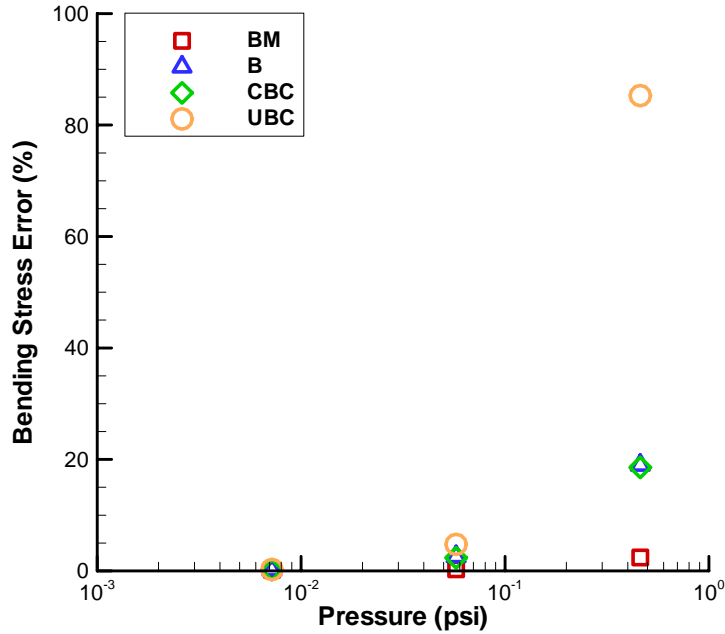


Figure 15: Quasi-static bending stress error integrated along the beam span.

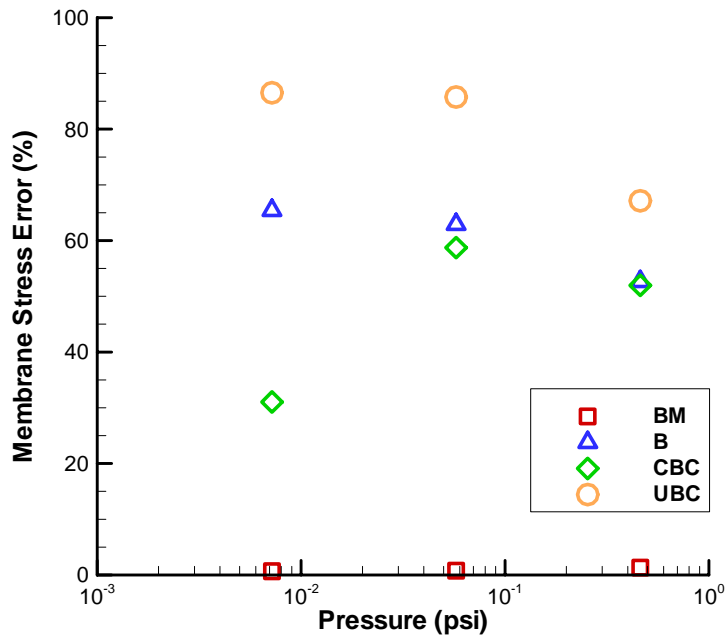


Figure 16: Quasi-static membrane stress error integrated along the beam span.

To summarize the findings from the quasi-static analysis, only the BM basis was able to capture the transverse and membrane displacements, and the bending and membrane stresses with high accuracy. The errors associated with the B, CBC, and UBC bases are generally smaller for the

transverse displacement and bending stress than they are for the membrane displacement and membrane stress. The errors associated with the membrane displacement and stress are so gross that the B, CBC and UBC bases are deemed unsuitable for their prediction for structures exhibiting nonlinear bending-membrane coupling. Consequently, if the membrane contribution is significant relative to that of bending, the B, CBC and UBC bases will also not be suitable. Therefore, some assessment of the membrane contribution must be made via an alternative analysis before blind application of the B, CBC or UBC bases.

### 3.3. RANDOM ACOUSTIC RESPONSE

For the nonlinear random response investigation, the beam was subjected to a uniformly distributed acoustic loading with a bandwidth of 1500 Hz. Three loading levels were considered to span the response regime from essentially linear to highly nonlinear; a low overall sound pressure level of 128 dB (0.0072 psi RMS), a medium level of 146 dB (0.0576 psi RMS), and a high level of 164 dB (0.4608 psi RMS). Damping was chosen to be sufficiently high so that good comparisons could be made at the peaks of the PSD. A level of mass proportional damping was specified corresponding to 2.0% critical damping for the first symmetric bending mode. The damping specified was the same for both the reduced-order and physical DoFs simulation analyses. For the nonlinear modal simulation, a fixed time integration step of between 50  $\mu s$  (for the lowest excitation levels) and 2  $\mu s$  (for the highest excitation levels) was used.

#### 3.3.1 Load Generation and Ensemble Averaging

The same loading time history and ensemble averaging was used for the numerical simulation analysis in physical and modal coordinates. The loading time histories were generated by summing equal amplitude sine waves, each with random phase, within the specified bandwidth using a discrete inverse Fourier transform. This procedure was identical to that used in previous work [5] by the authors, so further details are omitted for brevity. The loading produced by this method has a Gaussian distribution. A sharp roll-off of the input spectrum practically eliminates excitation of the structure outside the frequency range of interest.

For each load level, ten ensembles of displacement and stress response were generated lasting 2.1384s each. The first 0.5s of each response record was discarded to remove the initial transient

response [5], resulting in response histories of 1.6384s in duration. For each simulation, the displacement and stress response was stored at every  $50 \mu s$ , giving time records of 32,768 points. A 32,768-point FFT was subsequently used to compute the power spectral density (PSD) function.

### 3.3.2 Results

The results shown are for the same bases considered in the quasi-static response analysis. The spectral results have been visually smoothed to more clearly observe the behavior. Transverse displacement PSDs are shown in Figure 17 for the medium loading of 146 dB. For this level, all modal bases agree well with the numerical simulation in physical DoFs, with the most significant differences at the third and fourth mode for the B, CBC and UBC bases. At this level, the transverse displacements obtained by the B and CBC bases are essentially the same.

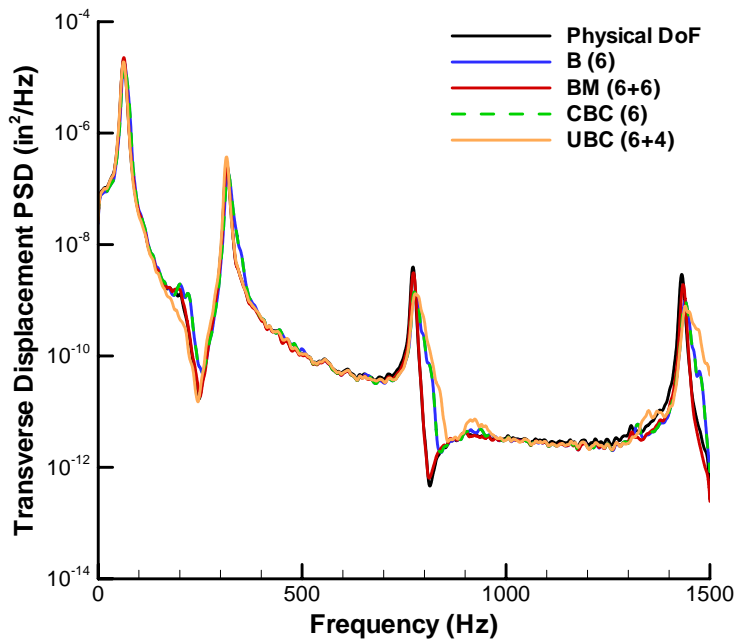


Figure 17: Quarter-span transverse displacement PSD of beam at 146 dB.

The membrane displacement PSDs for this load level, shown in Figure 18, offer a different perspective. The BM basis is the only one to compare well with the physical DoFs simulation results. The CBC basis is inaccurate on two accounts; the magnitude is clearly incorrect and the shape of the frequency response mimics that of the bending response in Figure 17. Like the quasi-static response, the UBC basis over-predicts the response amplitude. Though the loading

spectrum falls off sharply at 1500 Hz, the membrane displacement response obtained using physical DoFs simulation and nonlinear modal simulations with B, BM, and UBC bases, extend to twice that frequency because of period doubling (not shown). The membrane displacement response computed using the CBC basis does not exhibit period doubling.

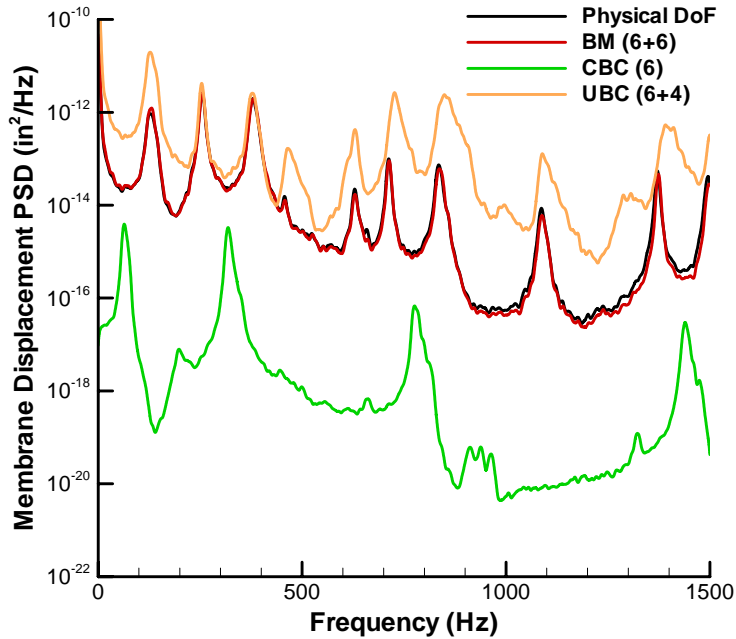


Figure 18: Quarter-span membrane displacement PSD of beam at 146 dB.

The bending stress PSDs at 146 dB are shown in Figure 19. The BM basis compares very well across the frequency range, even at the anti-resonances. The B and CBC stress PSDs are essentially the same, and under-predict the third and fourth resonances. The UBC basis is similar, but also under-predicts the fundamental. The membrane stress PSDs are shown in Figure 20. The BM basis compares remarkably well with the physical DoFs simulation. Again, the B, CBC, and UBC results fall on either side of the physical DoFs simulation, while above that frequency they all over-predict the response.

At the highest loading of 164 dB, the transverse displacement PSD exhibits the peak spreading and shifting characteristic of spring hardening nonlinearity, see Figure 21. For this case, the bending-only and CBC bases indicate a higher degree of nonlinearity than the physical DoFs simulation results, as evidenced by the first and second peaks shifted to higher frequencies, greater broadening, and smaller magnitudes. Results from the UBC basis were not available due

to the aforementioned numerical integration problems. The BM basis results compare well across the frequency range, with some loss of peak response in the third peak.

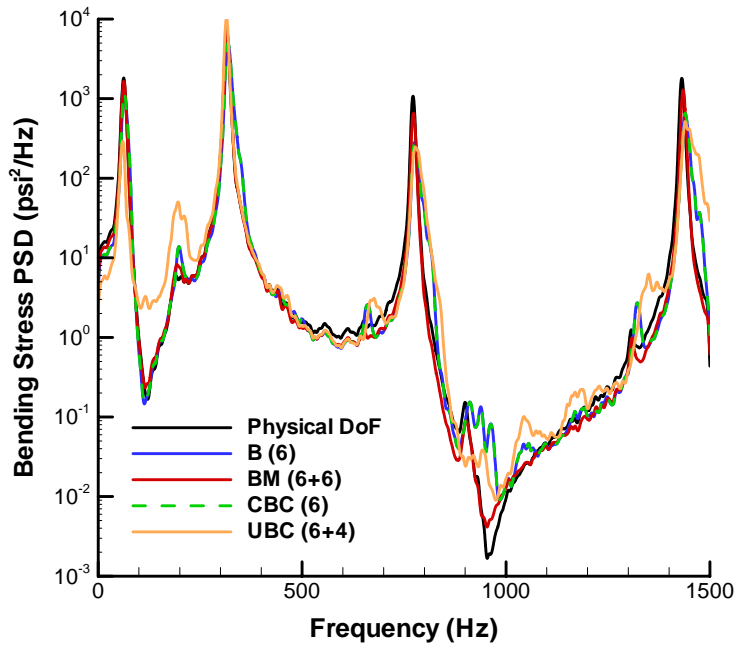


Figure 19: Quarter-span bending stress PSD of beam at 146 dB.

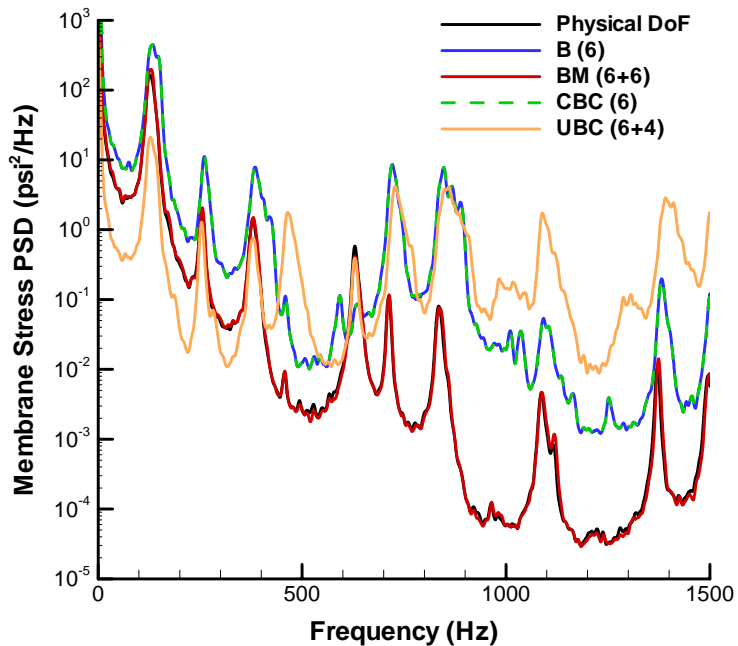


Figure 20: Quarter-span membrane stress PSD of beam at 146 dB.

The membrane behavior shown in Figure 22 follows the observations made at 146 dB. The excellent agreement between BM basis and physical DoFs simulation results demonstrate the efficacy of the BM basis in the highly nonlinear dynamic response regime.

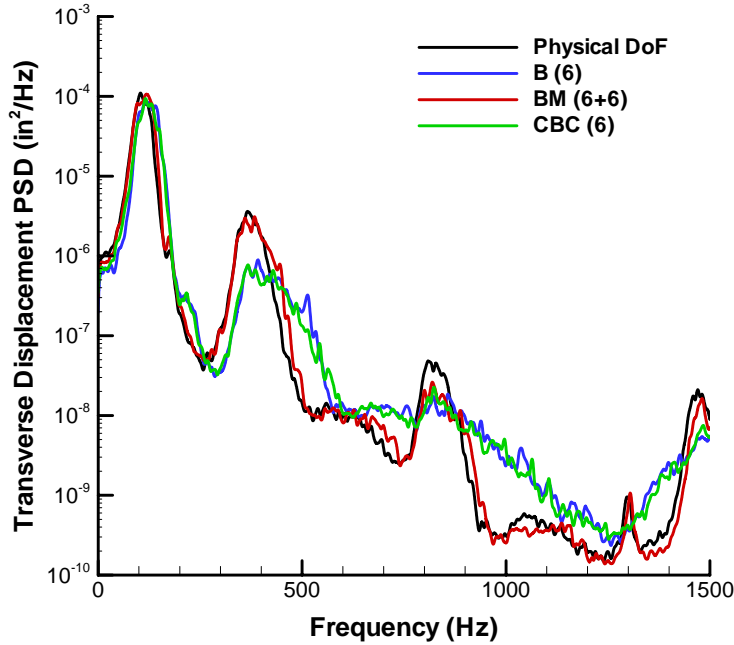


Figure 21: Quarter-span transverse displacement PSD of beam at 164 dB.

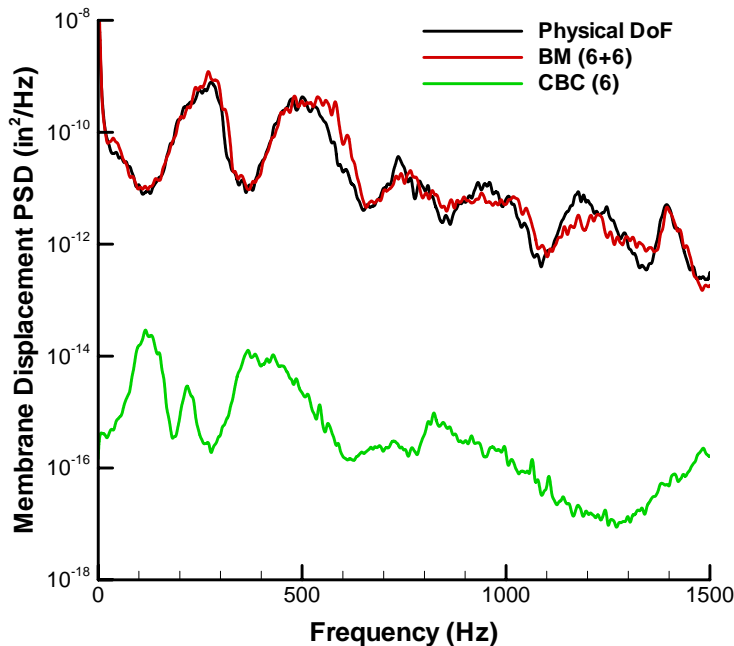


Figure 22: Quarter-span membrane displacement PSD of beam at 164 dB.

Bending and membrane stress PSDs at 164 dB are shown in Figure 23 and Figure 24, respectively. The BM basis most closely compares with the physical DoFs simulation bending

stress across the frequency range, with some loss in amplitude response in the peak near 850 Hz. The bending-only and CBC bases significantly under-predict the bending stress of the first and second modes and, above about 950 Hz, indicate different character than the BM basis and physical DoFs results.

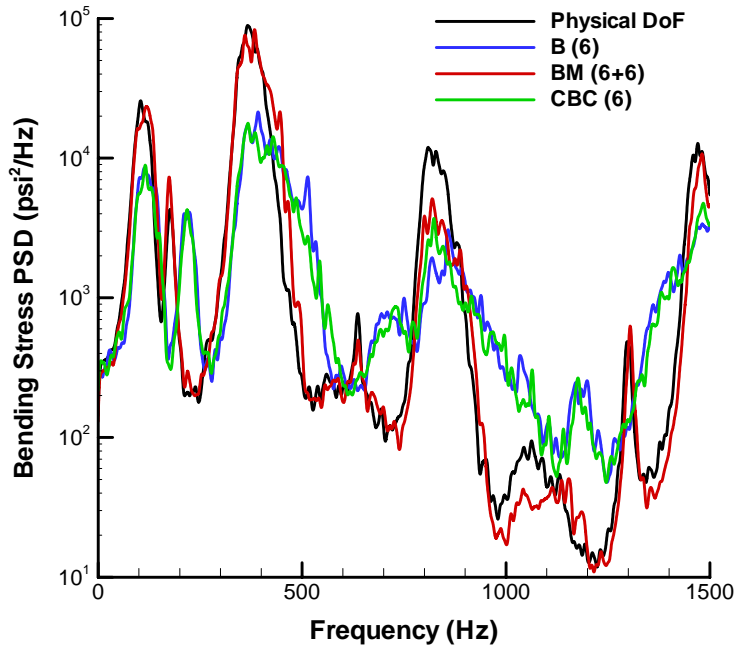


Figure 23: Quarter-span bending stress PSD of beam at 164 dB.

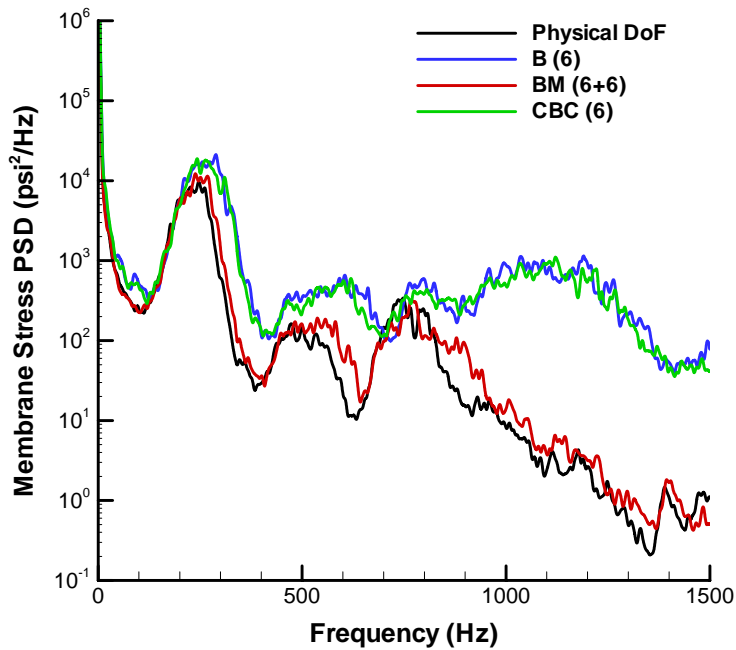


Figure 24: Quarter-span membrane stress PSD of beam at 164 dB.

In Figure 24, the BM basis results compare favorably with the physical DoFs simulation results across the frequency range. The bending-only and CBC bases over-predict the membrane stress magnitude and width of the first peak. Above about 750 Hz, the character substantially differs from the physical DoFs results.

To quantify the error in the root-mean-square of the response, the following measure was used:

$$\% \text{ Error} = \left( \frac{RMS(\text{Physical DoFs}) - RMS(\text{Reduced Order})}{RMS(\text{Physical DoFs})} \right) \times 100. \quad (11)$$

The error in RMS response is an indicator of the error over the entire frequency range, and hence is not capable of representing the differences in the spectral character. Figure 25 and Figure 26 present the error estimates for transverse and membrane displacements, respectively, and Figure 27 and Figure 28 present the error estimates for bending and membrane stresses, respectively. While the RMS transverse displacement is estimated with least accuracy by the BM basis, it should be noted that this is primarily attributable to differences in the fundamental mode, which dominates the response. The 7% error in the RMS displacement transverse displacement is considered acceptable for a random analysis, particularly at the high nonlinear levels where the width of the confidence intervals is large [5].

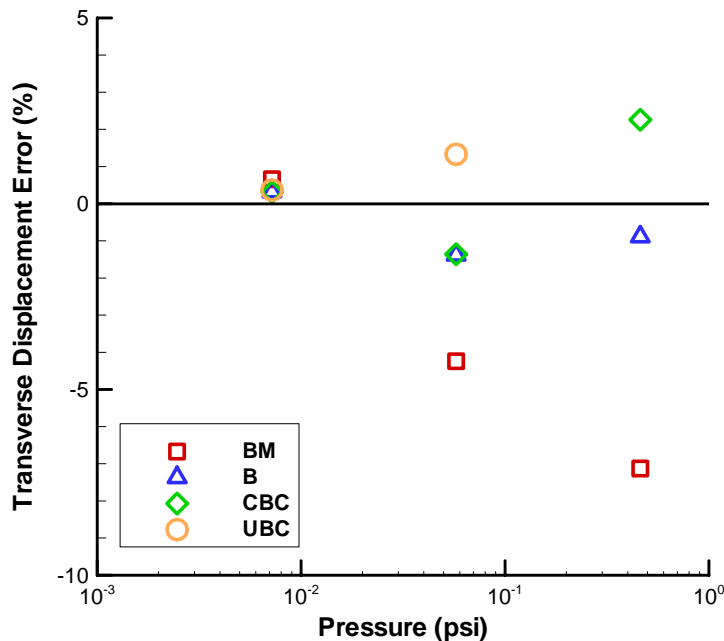


Figure 25: Error in random acoustic RMS transverse displacement response at beam 1/4 span.

On the other hand, the RMS membrane displacement is captured most accurately by the BM basis. As shown in Figure 18 and Figure 22, the membrane displacement is dominated by the zero frequency component, which results from the fact that the membrane displacement oscillates between zero and some positive value. For the error in RMS membrane displacement, the CBC and UBC bases can be off by as much as one order of magnitude.

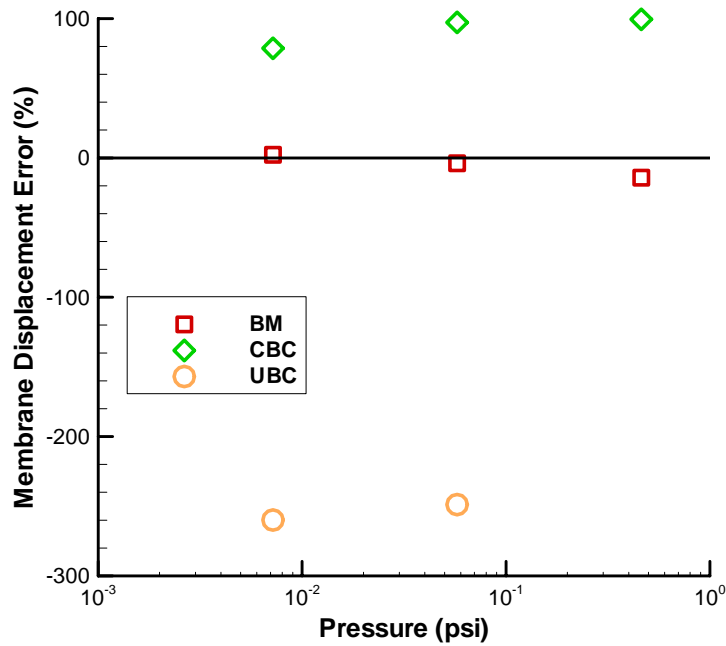


Figure 26: Error in random acoustic RMS membrane displacement response at beam  $\frac{1}{4}$  span.

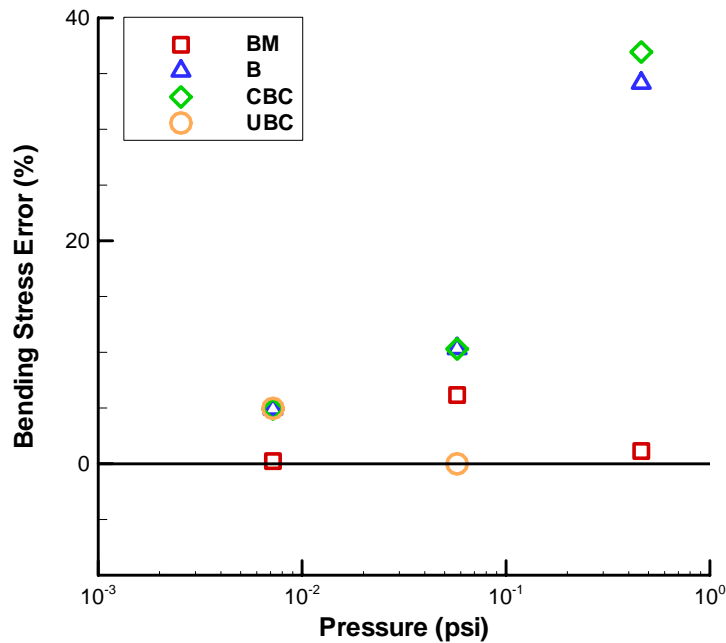


Figure 27: Error in random acoustic RMS bending stress response at beam  $\frac{1}{4}$  span.

With regard to the stress response in Figure 27 and Figure 28, the BM basis provides the most accurate stress response, with a somewhat higher error in the bending stress at the medium load level. Again, this is likely a reflection of differences in the peak values. Bases B and CBC provide the lowest quality of stress estimation. For the bending stress, the RMS value is affected by several peaks of comparable magnitude, while the RMS membrane stress is dominated by the zero frequency component (see Figure 20 and Figure 24).

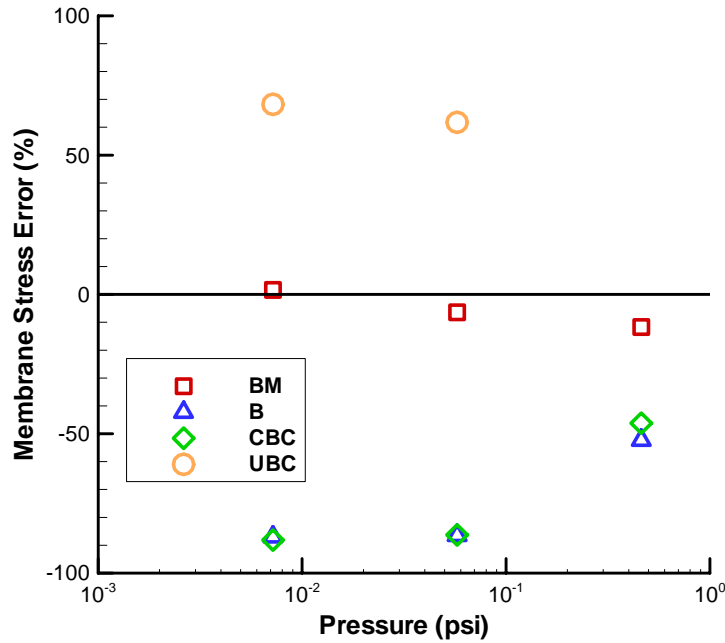


Figure 28: Error in random acoustic RMS membrane stress response at beam  $\frac{1}{4}$  span.

#### 4. NONLINEAR STATIC AND RANDOM ACOUSTIC RESPONSE OF A PLATE

A plate was next considered to help understand the complexities of modal basis selection for a two-dimensional structure. Since the beam results presented in Sec. 3 indicated that the BM basis was superior over all the other basis variants considered, the nonlinear reduced-order results for the plate were computed using only the BM basis.

The plate measured 14-in. x 10-in. x 0.04-in. ( $x \times y \times h$ ) with the aluminum material properties introduced in Sec. 2.2.3. The boundary conditions were simply supported on all sides. Specifically, along the 14-in. sides (in the  $x$ -direction), the transverse displacement DoF ( $w$ ), the membrane displacement DoF in the  $y$ -direction ( $v$ ), and the rotational DoF about the  $y$ -axis were

constrained. Along the 10-in. sides (in the  $y$ -direction), the  $w$  DoF, the membrane displacement DoF in the  $x$ -direction ( $u$ ), and the rotational DoF about the  $x$ -axis were constrained.

The ABAQUS model used for simulation in physical DoFs consisted of 8960 S4R elements measuring 0.125-in. x 0.125-in. The S4R element has one integration point, compared to four for the S4 element, and is required in the ABAQUS explicit analysis. The double precision explicit integration scheme with adaptive time step was used for both quasi-static and random acoustic response analyses.

For the reduced-order analysis, the MSC.NASTRAN model used consisted of 8960 CQUAD4 elements measuring 0.125-in. x 0.125-in. Up to the first twelve (eigenvectors 1, 4, 8, 11, 12, 19, 22, 23, 28, 31, 35, and 40) doubly symmetric bending modes, i.e., symmetric in both  $x$ - $y$  plan-form directions, were included in the basis. These occurred at natural frequencies 58, 216, 367, 524, 531, 838, 985, 1003, 1140, 1308, 1452, and 1633 Hz, respectively. For the membrane modes, the selection was guided by the previous experience gained from the beam analysis, that is, membrane displacement components were either both anti-symmetric, or one was anti-symmetric and the other was zero. Up to the first twelve membrane modes were included (eigenvectors 426, 438, 618, 638, 778, 798, 894, 917, 935, 1142, 1152, and 1184). These occurred at natural frequencies of 15.2, 15.4, 21.2, 21.9, 26.1, 26.6, 29.6, 30.3, 30.8, 36.7, 36.9, and 37.9 kHz, respectively.

#### 4.1. QUASI-STATIC RESPONSE

The effect of modal truncation on the quasi-static displacement results was first considered. The applied loading had a quasi-steady characteristic, as described in Sec. 3.2.1, and was uniformly distributed over the plate surface. Three BM modal bases were used; an 8-mode basis consisting of the first four symmetric bending modes and first four anti-symmetric membrane modes (4+4), a 16-mode basis consisting of the first eight symmetric bending modes and first eight anti-symmetric membrane modes (8+8), and a 24-mode basis consisting of the first twelve symmetric bending modes and first twelve anti-symmetric membrane modes (12+12). By analogy to the beam results, plate displacement results are presented at the  $\frac{1}{4}$  -  $\frac{1}{4}$  span location (3.5-in. from the boundary in the  $x$ -direction, and 2.5-in. from the boundary in the  $y$ -direction).

The transverse displacement ( $w$ ) error and both membrane displacement ( $u$  in the  $x$ -direction,  $v$  in the  $y$ -direction) errors were computed as per Equation (9), and are shown in Table 6 for a range of loadings. It is seen that for the lowest quasi-static loading of  $5.801 \times 10^{-4}$  psi, the modal truncation has little effect on the displacement accuracy, and results computed with eight, sixteen, and twenty-four basis vectors are essentially the same. The center displacement at this level was  $w_{\max}/h = 0.016$ . As the quasi-static loading increases, the effect of nonlinearity increases, with a center displacement of  $w_{\max}/h = 0.408$  for the  $1.856 \times 10^{-2}$  psi load, and  $w_{\max}/h = 1.545$  for the 0.297 psi load. The number of basis vectors used plays an increasingly important role as the load increases. The effect is more pronounced in the membrane displacement component errors than it is in the transverse displacement error.

Table 6: Plate quasi-static displacement errors at ( $1/4, 1/4$ ) location, %.

	$w$	$u$	$v$
<b><math>5.801 \times 10^{-4}</math> psi</b>			
BM (12+12)	-2.16	-4.32	-4.79
BM (8+8)	-2.17	-4.39	-0.18
BM (4+4)	-2.55	-2.89	-1.31
<b><math>1.856 \times 10^{-2}</math> psi</b>			
BM (12+12)	-1.52	-3.52	-3.41
BM (8+8)	-1.41	-2.55	2.54
BM (4+4)	1.34	4.23	7.44
<b>0.297 psi</b>			
BM (12+12)	-0.48	-3.89	0.56
BM (8+8)	1.06	5.34	13.81
BM (4+4)	4.28	17.25	16.79

In the process of selecting membrane modes for the basis, the lowest anti-symmetric modes were included without regard for the number of periods in the  $x$  and  $y$ -directions. Since the  $y$ -dimension is shorter, it is also stiffer. This means that membrane modes corresponding to this direction will generally have higher natural frequencies than the ones associated with membrane motion in the longer plate dimension. Of the first 12 membrane modes used, the maximum number of periods in the  $x$ -direction was four, while the maximum number in the  $y$ -direction was two. Consequently, it is expected that modal reduction utilizing 12 membrane modes for the plate is less accurate than the best modal reduction for the beam utilizing 6 membrane modes, as the latter had six periods along the beam's span. The conclusion is that the reduced-order

analysis for a two-dimensional structure requires an expanded modal basis relative to a one-dimensional structure of comparable characteristic length and excitation bandwidth.

#### 4.2. RANDOM ACOUSTIC RESPONSE

For the random analysis, a uniformly distributed acoustic load with a bandwidth of 1024 Hz was applied. Two loading levels were considered; a low overall sound pressure level of 106 dB ( $5.801 \times 10^{-4}$  psi RMS) and a high level of 164 dB (0.297 psi RMS). Similar to the beam studies, a mass proportional 2% critical damping corresponding to the fundamental mode was prescribed. The displacement error corresponding to the random plate response in an RMS sense, as per Equation (11), is presented in Table 7 for the two loadings levels.

Table 7: Plate random displacement errors at  $(\frac{1}{4}, \frac{1}{4})$  location, %.

	$w$	$u$	$v$
<b>106 dB</b>			
BM (12+12)	-0.32	-10.17	-2.55
BM (8+8)	-0.32	-10.13	-2.57
BM (4+4)	-0.40	-10.97	-2.56
<b>160 dB</b>			
BM (12+12)	4.00	-38.68	-26.43
BM (8+8)	14.63	46.35	48.02
BM (4+4)	20.64	63.04	52.00

For the 106 dB level, which results in a linear response regime with  $w_{\max}/h = 0.024$ , the effect of modal truncation is negligible; 8, 16, and 24 basis vectors analyses yield essentially the same RMS error. As the excitation level is increased to 160 dB, the response becomes highly nonlinear with  $w_{\max}/h = 2.373$ . At this level, modal truncation starts playing a very important role and its effect is significantly magnified when compared to a quasi-static case. The quasi-static analysis performed utilizing 8 basis vectors (4+4) for the 0.297 psi load yielded a transverse displacement error of about 4%, while the random response analysis for the 160 dB load (0.297 psi RMS) required 24 basis vectors (12+12) to obtain comparable results. This trend was also observed in the results for the beam. Consistent with observations based on the quasi-static analysis, the error in the random transverse displacement is substantially less than the error in either component of the random membrane displacement.

## 5. CONCLUSIONS

Nonlinear modal simulation using an indirect nonlinear stiffness evaluation method has been shown to provide accurate predictions of nonlinear quasi-static and random response, when an appropriate basis is selected. When used in conjunction with direct numerical simulation for validation, the approach constitutes one of the few high-fidelity design options for nonlinear random vibration and high-cycle fatigue.

The following conclusions are limited to the class of problems considered, i.e. those exhibiting nonlinear bending-membrane coupling. Of the four modal basis variants considered, the bending and membrane modal basis was found to be the only one to accurately predict transverse and membrane displacement, and bending and membrane stress at any location on the structure. Its main drawback is that identification and selection of membrane modes is labor intensive even for the simple beam and plate structures considered.

The bending-only basis was the simplest amongst the variants in terms of the modal basis selection. However, the bending-only basis was incapable of computing membrane displacement response, and the accuracy of the membrane stress prediction was highly dependent on location. Further, it over-predicted the effects of nonlinearity on the random response.

For the combined bending-companion modal basis, there was no issue with regard to identifying the companion modes, and their inclusion did not increase the system size. However, there was no engineering rationale for selecting which initial imperfection shape to apply when computing the dynamic companion. It was found that results obtained using this basis were comparable to those obtained using the bending-only basis, except for the membrane displacement, which the latter was unable to predict. The random membrane displacement response did not exhibit period doubling, and was significantly reduced in amplitude relative to the physical DoFs simulation.

For the uncoupled bending-companion modal basis, there was also no engineering rationale for selecting which initial imperfection shape to apply when computing the dynamic companion. When computing the static companion, there was no engineering rationale for selecting which displacement or loading to apply. Both static and dynamic UBC bases indicated different

coupling between bending and companion modes than the coupling between bending and membrane modes for the BM basis. For both static and dynamic UBC bases, a numerical instability problem limited the number of companions that could be included in the basis, without the use of static condensation in modal coordinates. Finally, for the UBC dynamic basis, the membrane displacement and stress response prediction was highly dependent upon location.

Finally, with regard to two-dimensional structures, it was found that the number of basis vectors needed for an accurate response prediction in a highly nonlinear regime had to be considerably expanded as compared to one-dimensional structures.

## REFERENCES

- [1] Vaicaitis, R., "Recent advances of time domain approach for nonlinear response and sonic fatigue," *Structural Dynamics: Recent Advances, Proceedings of the 4th International Conference*, pp. 84-103, Southampton, UK, 1991.
- [2] Green, P.D. and Killey, A., "Time domain dynamic finite element modelling in acoustic fatigue design," *Structural Dynamics: Recent Advances, Proceedings of the 6th International Conference*, Vol. 2, pp. 1007-1025, Southampton, UK, 1997.
- [3] Caughy, T.K., "Equivalent linearization techniques," *Journal of the Acoustical Society of America*, Vol. 35, pp. 1706-1711, 1963.
- [4] Roberts, J.B. and Spanos, P.D., *Random vibration and statistical linearization*. New York, NY, John Wiley & Sons, 1990.
- [5] Rizzi, S.A. and Muravyov, A.A., "Comparison of nonlinear random response using equivalent linearization and numerical simulation," *Structural Dynamics: Recent Advances, Proceedings of the 7th International Conference*, Vol. 2, pp. 833-846, Southampton, UK, 2000.
- [6] Rizzi, S.A., "On the use of equivalent linearization for high-cycle fatigue analysis of geometrically nonlinear structures," *Structural Dynamics: Recent Advances, Proceedings of the 8th International Conference*, Southampton, UK, 2003.
- [7] Mei, C., Dhainaut, J.M., Duan, B., Spottswood, S.M., and Wolfe, H.F., "Nonlinear random response of composite panels in an elevated thermal environment," Air Force Research Laboratory, Wright-Patterson Air Force Base, OH, AFRL-VA-WP-TR-2000-3049, October 2000.
- [8] Przekop, A., "Nonlinear response and fatigue estimation of aerospace curved surface panels to combined acoustic and thermal loads," *Ph.D. Dissertation*, Old Dominion University, 2003.
- [9] Przekop, A., Guo, X., Azzouz, M.S., and Mei, C., "Reinvestigation of nonlinear random response of shallow shells using finite element modal formulation," *Proceedings of the 45th AIAA/ASME/ASCE/AHS/ASC Structures, Structural Dynamics and Materials Conference*, AIAA-2004-1553, Palm Springs, CA, 2004.
- [10] Hollkamp, J.J., Gordon, R.W., and Spottswood, S.M., "Nonlinear sonic fatigue response prediction from finite element modal models: a comparison with experiments,"

- Proceedings of the 44th AIAA/ASME/ASCE/AHS/ASC Structures, Structural Dynamics, and Materials Conference*, AIAA-2003-1709, Norfolk, VA, 2003.
- [11] Bathe, K.J. and Gracewski, S., "On nonlinear dynamic analysis using substructuring and mode superposition," *Computers and Structures*, Vol. 13, pp. 699-707, 1981.
- [12] McEwan, M.I., Wright, J.R., Cooper, J.E., and Leung, Y.T., "A finite element/modal technique for nonlinear plate and stiffened panel response prediction," *Proceedings of the 42nd AIAA/ASME/ASCE/AHS/ASC Structures, Structural Dynamics, and Materials Conference*, AIAA-2001-1595, Seattle, WA, 2001.
- [13] McEwan, M.I., Wright, J.R., Cooper, J.E., and Leung, Y.T., "A combined modal/finite element analysis technique for the dynamic response of a non-linear beam to harmonic excitation," *Journal of Sound and Vibration*, Vol. 243, No. 4, pp. 601-624, 2001.
- [14] Muravyov, A.A. and Rizzi, S.A., "Determination of nonlinear stiffness with application to random vibration of geometrically nonlinear structures," *Computers and Structures*, Vol. 81, No. 15, pp. 1513-1523, 2003.
- [15] Hollkamp, J.J. and Gordon, R.W., "Modeling membrane displacements in the sonic fatigue response prediction problem," *Proceedings of the 46th AIAA/ASME/ASCE/AHS/ASC Structures, Structural Dynamics and Materials Conference*, Austin, TX, 2005.
- [16] Mignolet, M.P., Radu, A.G., and Gao, X., "Validation of reduced order modeling for the prediction of the response and fatigue life of panels subjected to thermo-acoustic effects," *Structural Dynamics: Recent Advances, Proceedings of the 8th International Conference*, Southampton, UK, 2003.
- [17] Press, W.H., Teukolsky, S.A., Vetterling, W.T., and Flannery, B.P., "Numerical recipes, the art of scientific computing," CDROM v2.10, Cambridge University Press, 2002.
- [18] Radu, A.G., Yang, B., Kim, K., and Mignolet, M.P., "Prediction of the dynamic response and fatigue life of panels subjected to thermo-acoustic loading," *Proceedings of the 45th AIAA/ASME/ASCE/AHS/ASC Structures, Structural Dynamics and Materials Conference*, AIAA-2004-1557, Palm Springs, CA, 2004.

REPORT DOCUMENTATION PAGE			Form Approved OMB No. 0704-0188		
<p>The public reporting burden for this collection of information is estimated to average 1 hour per response, including the time for reviewing instructions, searching existing data sources, gathering and maintaining the data needed, and completing and reviewing the collection of information. Send comments regarding this burden estimate or any other aspect of this collection of information, including suggestions for reducing this burden, to Department of Defense, Washington Headquarters Services, Directorate for Information Operations and Reports (0704-0188), 1215 Jefferson Davis Highway, Suite 1204, Arlington, VA 22202-4302. Respondents should be aware that notwithstanding any other provision of law, no person shall be subject to any penalty for failing to comply with a collection of information if it does not display a currently valid OMB control number.</p> <p><b>PLEASE DO NOT RETURN YOUR FORM TO THE ABOVE ADDRESS.</b></p>					
1. REPORT DATE (DD-MM-YYYY)		2. REPORT TYPE		3. DATES COVERED (From - To)	
01- 12 - 2005		Technical Publication		Jun 2003 - Sept 2004	
4. TITLE AND SUBTITLE The Effect of Basis Selection on Static and Random Acoustic Response Prediction Using a Nonlinear Modal Simulation			5a. CONTRACT NUMBER		
			5b. GRANT NUMBER		
			5c. PROGRAM ELEMENT NUMBER		
6. AUTHOR(S) Stephen A. Rizzi (NASA) Adam Przekop (NIA)			5d. PROJECT NUMBER		
			5e. TASK NUMBER		
			5f. WORK UNIT NUMBER 23-794-40-4A		
7. PERFORMING ORGANIZATION NAME(S) AND ADDRESS(ES) NASA Langley Research Center Hampton, VA 23681-2199			8. PERFORMING ORGANIZATION REPORT NUMBER  L-19201		
9. SPONSORING/MONITORING AGENCY NAME(S) AND ADDRESS(ES) National Aeronautics and Space Administration Washington, DC 20546-0001			10. SPONSOR/MONITOR'S ACRONYM(S)  NASA		
			11. SPONSOR/MONITOR'S REPORT NUMBER(S)  NASA/TP-2005-213943		
12. DISTRIBUTION/AVAILABILITY STATEMENT Unclassified - Unlimited Subject Category 39 Availability: NASA CASI (301) 621-0390					
13. SUPPLEMENTARY NOTES An electronic version can be found at <a href="http://ntrs.nasa.gov">http://ntrs.nasa.gov</a>					
14. ABSTRACT An investigation of the effect of basis selection on geometric nonlinear response prediction using a reduced-order nonlinear modal simulation is presented. The accuracy is dictated by the selection of the basis used to determine the nonlinear modal stiffness. This study considers a suite of available bases including bending modes only, bending and membrane modes, coupled bending and companion modes, and uncoupled bending and companion modes. The nonlinear modal simulation presented is broadly applicable and is demonstrated for nonlinear quasi-static and random acoustic response of flat beam and plate structures with isotropic material properties. Reduced-order analysis predictions are compared with those made using a numerical simulation in physical degrees-of-freedom to quantify the error associated with the selected modal bases. Bending and membrane responses are separately presented to help differentiate the bases.					
15. SUBJECT TERMS Reduced-order numerical simulation; Geometric nonlinear response; Nonlinear stiffness evaluation					
16. SECURITY CLASSIFICATION OF:			17. LIMITATION OF ABSTRACT	18. NUMBER OF PAGES	19a. NAME OF RESPONSIBLE PERSON
a. REPORT	b. ABSTRACT	c. THIS PAGE			STI Help Desk (email: <a href="mailto:help@sti.nasa.gov">help@sti.nasa.gov</a> )
U	U	U	UU	46	19b. TELEPHONE NUMBER (Include area code) (301) 621-0390